ACS OMEGA

Open Access

http://pubs.acs.org/journal/acsodf

Review

Light Addressable Potentiometric Sensors for Biochemical Imaging on Microscale: A Review on Optimization of Imaging Speed and Spatial Resolution

Jiezhang Luo, Shibin Liu,* Yinhao Chen, Jie Tan, Wenbo Zhao, Yun Zhang, Guifang Li, Yongqian Du, Yaoxin Zheng, Xueliang Li, Huijuan Li, and Yue Tan

Cite This: *ACS Omega* 2023, 8, 42028−42044

Read Online

ACCESS | Metrics & More | Article Recommendations

ABSTRACT: Light addressable potentiometric sensors (LAPS) are a competitive tool for unmarked biochemical imaging, especially imaging on microscale. It is essential to optimize the imaging speed and spatial resolution of LAPS since the imaging targets of LAPS, such as cell, microfluidic channel, etc., require LAPS to image at the micrometer level, and a fast enough imaging speed is a prerequisite for the dynamic process involved in biochemical imaging. In this study, we discuss the improvement of LAPS in terms of imaging speed and spatial resolution. The development of LAPS in imaging speed and spatial resolution is demonstrated by the latest applications of biochemistry monitoring and imaging on the microscale.

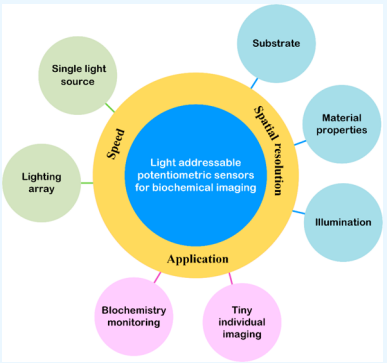

1. INTRODUCTION

A variety of analytical tools are designed for biochemical detection, such as fluorescence imaging, microelectrode array, plasmonic-based electrochemical impedance microscopy (P-EIM), ion-sensitive field-effect transistor (ISFET) array, field-effect-addressable potentiometric sensor (FAPS), light-addressable potentiometric sensors (LAPS), etc. Fluorescence imaging, which distinguishes the analytes from the environment through adding the label reagent, has been widely used for biochemical imaging. However, the label reagents will influence the cellular activities or chemical compositions and introduce some irrelevant factors during the experiment. Moreover, the label reagents usually have phototoxicity and photobleaching impacts, which make it hard to meet the increasing demand for environmentally friendly characteristics.[1] As the development of biochemistry continues, label-free technology has become required for detection.

Microelectrode array, as a sort of label-free technology, is widely used for detecting the activities of neurons and cardiomyocytes. Increasing microelectrode density is a practical strategy to handle the problem of high electrode impedance and promotes spatial resolution to the subcellular level. Nevertheless, this method has its limitations. The plasma membranes of cells cannot expend to the narrow spaces among the pillars of extracellular microelectrodes.[2] In another case of intracellular microelectrode, its impedance property is excellent, but the intracellular configuration will be influenced at the same time.[3]

To obtain more abundant details about biochemical analysis, the detection mode has evolved from overall detection to imaging. Plasmonic-based electrochemical impedance imaging (P-EIM) is another type of label-free technology with high sensitivity to the change of surface charge and can be applied to detect the action potential of a neuron,[4] monitor DNA charge regulations,[5] measure the binding kinetics of a small molecule on a protein.[6] ISFET,[7] as a field-effect semiconductor sensor, can be applied for studying various reaction mechanisms, such as enzymatic reactions, DNA pairing, etc., by modifying different sensitive membranes. On the ISFET array, FAPS is proposed later. FAPS integrates sensitive units and employs the crossing back-gate electrodes as an addressing method.[8,9] However, the test sites of ISFET array or FAPS are fixed after fabrication, and the increase of sites density will be followed by the lift of manufacturing cost and signal processing complexity because the spatial resolution of FABS relies on its site density.

Received: July 4, 2023
Revised: October 12, 2023
Accepted: October 17, 2023
Published: November 3, 2023

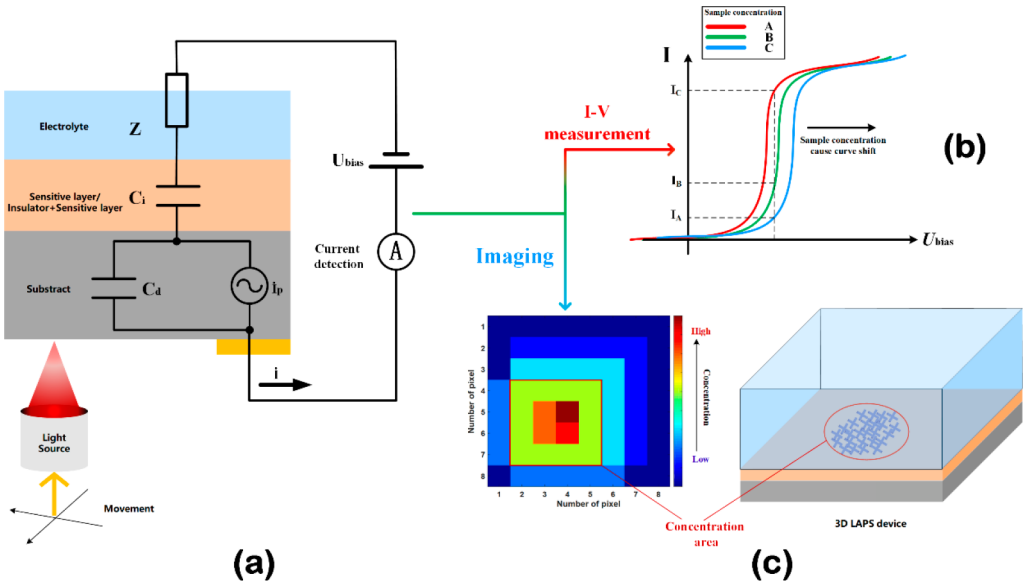

Figure 1. (a) Structure and (b) principle of concentration measurement and (c) chemical imaging.

Table 1. Characteristics of Label-Free Biochemical Imaging Technology

Technology	Illumination	Back-electrode	Detection target	Ref
P-EIM	Polarized light	No	Action potential of neuron, DNA charge regulations, binding kinetics of small molecule on protein	4, 6
FAPS	No	Electrode array	Detection target of ISFET, such as various ions, macromolecules, activity of cells, etc.	8, 9
LAPS	AC light beam or lighting array	Single electrode	Various ions, macromolecules, activity of cells, shape of single cell, bacterial colony, enzymatic reaction, etc.	14, 30

LAPS is an electrochemical sensor with a simple stacked structure based on the potential measurement principle. The working mechanism of LAPS can be analyzed by the semiconductor field-effect principle[10] and photoelectric effect of semiconductors.[11] Applying a suitable bias between the reference electrode and output electrode will cause a depletion region appearing inside the semiconductor. AC modulated illumination light irradiation on the semiconductor layer of the LAPS leads to photogenerated current inside the semiconductor. Illumination with alternating-modulation applied to the substrate will force the generated photocurrent that appears in the semiconductor of LAPS. The mechanism of the generated photocurrent has been analyzed in detail.[12] The simple circuit model of LAPS is shown in Figure 1a, where the relationship between the generated photocurrent $\dot{I}_p$ and the external output $\dot{I}$ is[13]

$$\dot{I} = \dot{I}_p \cdot \frac{C_i}{C_i + C_d} \quad (1)$$

The capacitance of the depletion region C_d is affected by the thickness of the depletion region. C_i is the capacitance of insulation. Therefore, the amplitude of the external current $\dot{I}$ can reflect the concentration of the measured substance. As shown in Figure 1b, the change of the concentration will cause a lateral shift in the bias voltage−current (V−I) curve. Assuming the bias voltage remains constant, the concentration change is reflected as the increase or decrease of the amplitude of external current $\dot{I}$. The potential between the electrolyte and the insulating layer is called the electrolyte/insulated gate interfacial potential, which can be related to the concentration of the measured substance through the Nernst equation. The concentration of the measured substance can be directly related to the interface potential, such as the relationship between the H^+ ion concentration and the interface potential between electrolyte/silicon nitride. In some cases, the concentration of the measured substance indirectly affects the interface potential, such as LAPS used for detecting DNA, where the binding of DNA to the target changes the pH value of the solution and influences the interface potential. Because photocarriers are generated only at the point of illumination, LAPS can provide flexible local measurements, where the measurement position and range are determined by illumination. As shown in Figure 1c, chemical images are obtained by scanning an entire substrate under a fixed bias voltage. The color of each position in the chemical image represents the photocurrent magnitude at the corresponding position of the sensor plate. Chemical images can illuminate the distribution of the concentration for the measured substance in space intuitively.

To some extent, LAPS retains several merits of potential sensors (ISFET, EIS capacitor, etc.), such as high measurement speed, high sensitivity, a wide range of applications, etc. Therefore, LAPS has good universality in the field of analysis science. In the past 30 years, LAPS has been applied in multiple aspects, such as disease diagnosis,[14,15] microbiology,[16−18] research of cell activity,[19−22] food safety,[23,24] pharmaceutical,[25,26] etc. A lot of application systems have been derived based on LAPS, such as electronic tongue,[27,28] integrated detection system,[29,30] etc.

Compared with the biochemical imaging technologies mentioned before, LAPS has the same advantage of free-label property with P-EIM, FAPS, and its addressing method of

https://doi.org/10.1021/acsomega.3c04789
ACS Omega 2023, 8, 42028−42044

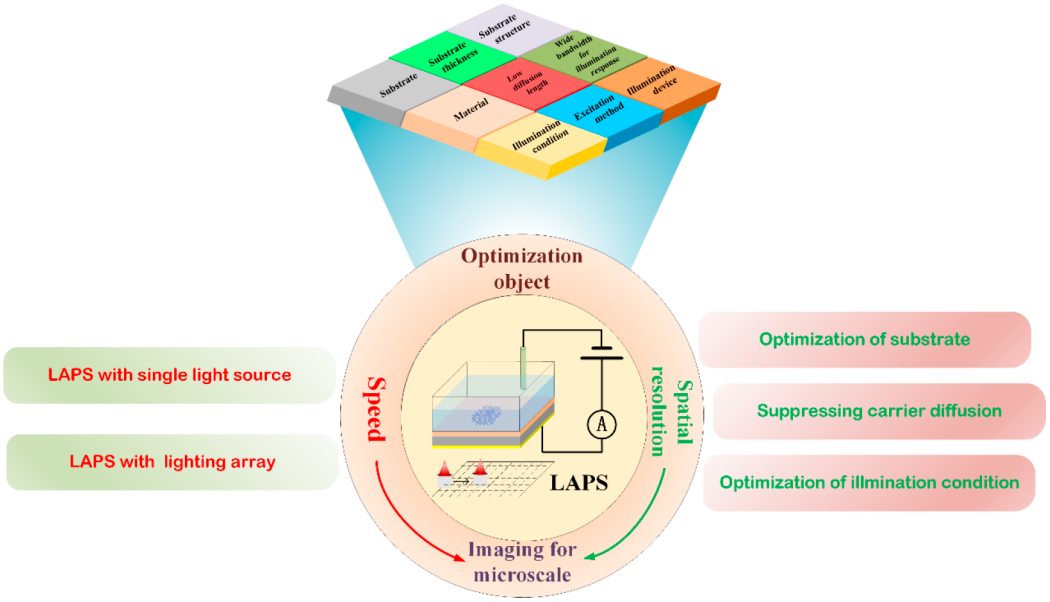

Figure 2. An overview of main topic about LAPS for biochemical imaging on microscale.

illumination has much more flexibility. The technical details of LAPS and other label-free imaging technologies are summarized in Table 1.

Researchers have paid attention to LAPS since it was first proposed[31] because of its outstanding advantages for biochemical detection: the flexibility measurement mechanism based on light addressing and label-free detection method. So far, a large number of applications based on LAPS have been developed.[32−43] The application modes of LAPS can be roughly divided into three types. The first is overall measurement of various biological or chemical samples such as DNA,[32] enzymes,[33,34] diabetes markers,[14,35] cancer markers,[15,20] ATP,[36] bacteria,[16,18] etc. The second type is to use multiple sensitive membranes to regionalize the surface modification of the sensor surface to achieve simultaneous monitoring of multiple substances on the same sensor, such as electron receptors,[37,38] cell metabolism monitoring,[39,40] extracellular acidification monitoring,[41] light-addressable DNA chips,[42] etc. The third type is to combine the addressing moving light source to carry out two-dimensional imaging on the sensor surface at the microscale, such as LAPS imaging system (measuring pH,[43] urea,[34] etc.), scanning photoinduced impedance microscopy (SPIM),[44−46] photoelectrochemical imaging system (PEIS),[47,48] scanning electrochemical photometric sensor (SEPS),[49] and light-addressable square wave voltammetry (LASWV) used for monitoring enzymatic reaction,[50] etc.

In order to gain a deeper understanding of the microworld, two-dimensional imaging systems based on LAPS suitable for microscale observations are developing constantly. Imaging speed and spatial resolution of LAPS determine the ability of a two-dimensional imaging system based on LAPS. In many cases, the process of chemical reactions or response of microorganisms is fast and requires the imaging speed to keep up with it. On the other hand, in order to understand the surface distribution of the detection target accurately, the imaging system based on LAPS needs to provide a high-resolution image. The development trend for imaging systems based on LAPS is high-speed and microscale imaging. Therefore, designing an imaging system that supports both high-speed and high-resolution imaging is still a research hotspot in the field of LAPS due to practical needs.

Here, we less discuss other fields, such as sensitivity, linearity, and so on. As shown in Figure 2, we have mainly reviewed the application of LAPS in the field of biochemical imaging in this work, which focuses on technology improvements relative on imaging speed and spatial resolution for LAPS. First, the progress of rapid imaging technologies applied in LAPS imaging systems, including the application of LAPS rapid imaging in the field of biochemistry and the achievements obtained in LAPS imaging speed, is reviewed. LAPS imaging speed optimization of LAPS mainly includes the optimization of LAPS imaging systems with a single light source and lighting array. Then, the imaging applications of high-resolution LAPS, such as cell imaging, microbial imaging, and enzymatic reaction observation, are introduced. Detailed introductions about methods for improving LAPS imaging resolution, such as substrate optimization and active suppression of carrier diffusion, are given. Finally, a simple summary about the development of microscale-biochemistry imaging based on LAPS is given. The future developments of LAPS imaging systems are predicted.

2. RAPID IMAGING TECHNOLOGY OF LAPS

2.1. Improvement of Imaging Speed. It can be assumed that the number of pixels in the chemical image obtained by LAPS is $n_x \times n_y$, where n_x and n_y are the numbers of pixels per row and column, respectively. Therefore, the total sampling time of chemical images T_{total} can be described as

$$T_{total} = T_{measure}\frac{n_x n_y}{n_{measure}} \quad (2)$$

$T_{measure}$ represents the time between the start of the measurement process and the finish of light beam movement. $n_{measure}$ represents the number of pixels processed during a measurement process.

It can be simply assumed that $T_{measure}$ is the time of a measurement process, which is influenced by many factors such as illumination frequency, measurement mode (constant

https://doi.org/10.1021/acsomega.3c04789
ACS Omega 2023, 8, 42028−42044

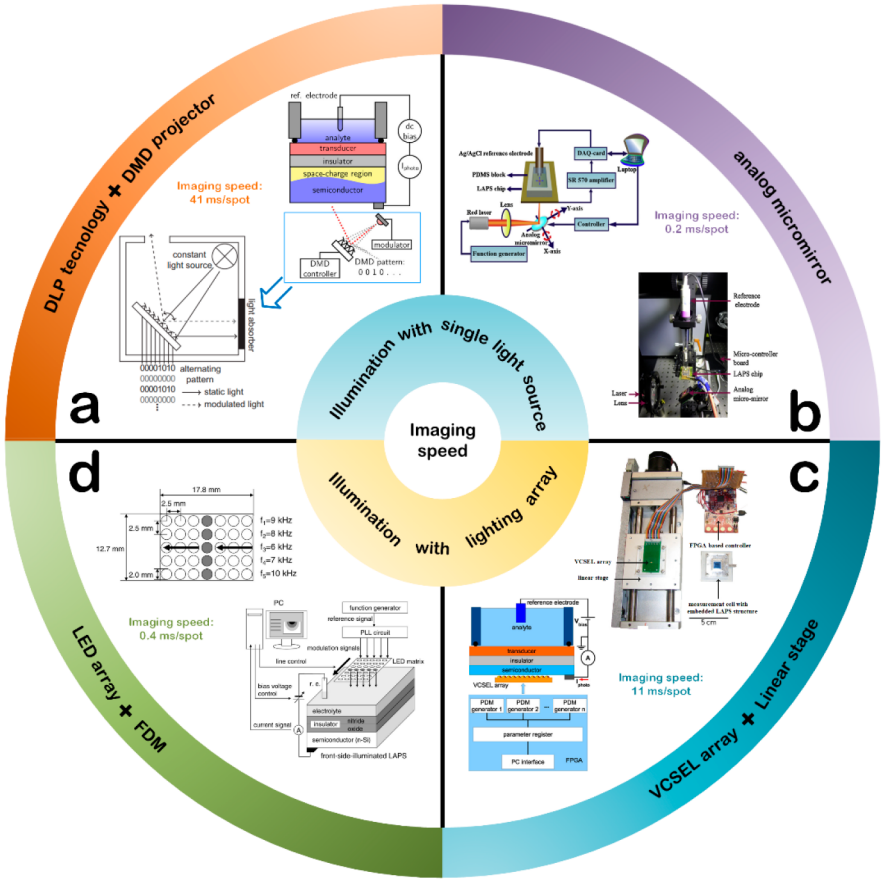

Figure 3. Four typical types of light source based on LAPS imaging system. (a) DLP technology controlling the DMD projector to finish moving the single light source. Reproduced with permission from ref 52. Copyright 2012 Elsevier. (b) Single light source providing a light beam moved by an analog micromirror system. Reproduced with permission from ref 58. Copyright 2014 Elsevier. (c) Light source being a lighting array based on VCSEL diodes combined with the linear stage. Reproduced with permission from ref 59. Copyright 2011 Elsevier. (d) LED array including 7 × 5 LEDs used to illuminate the substrate from the front side. Reproduced with permission from ref 61. Copyright 2013 Elsevier.

bias mode, voltage tracking mode), movement speed of the light source, etc. Compared with the voltage tracking mode, LAPS working on the constant bias mode needs fewer sampling points in the V−I curve, which leads to smaller $T_{measure}$. A traditional imaging system based on LAPS scans the substrate for imaging with a single light source, which obtains the pixel one by one.[51−58] The system with a single light source only obtains pixel data per measurement process ($n_{measure}$ = 1). In recent years, imaging systems employing light arrays have been proposed to provide rapid imaging.[59−63] The lighting array can simultaneously emit multiple light beams, where the light intensity of each light beam is modulated with specific frequencies. Because fast Fourier transform (FFT) technology can help extract components with different frequencies from photocurrent, pixels with the number of light beams can be obtained in a measurement process ($n_{measure}$ = the number of light beams).

2.1.1. Optimization of LAPS Imaging System with Single Light Source. At the early stage of imaging systems based on LAPS, a mechanical platform was used to move the light source. The power source of the mechanical platform is a stepper motor, which is the main reason for a reduction in imaging speed. The mechanical platform can provide high-precision displacement for a light source because the repeated positioning accuracy of the mechanical platform is less than 1 μm. However, as shown in eq 2, the mechanical platform combines with a single light source to obtain pixels data one by one. The displacement speed of the mechanical platform is slow and limits the imaging speed of LAPS. For example, Motoi Nakao achieves pH distribution images to observe colonies of *Saccharomyces cerevisiae* indirectly,[51] where the image size and imaging speed are 128 × 128 pixels and 110 ms/spot, respectively. As shown in Figure 3a, Wagner et al. propose the imaging system using a digital micromirror device (DMD) projector as the light source.[52] With the help of digital light processing (DLP) technology, the DMD projector can provide illumination with different spot sizes and positions through fast switching mirrors, which have a switching speed of 1440 Hz. Because the displacement of the light source for the DMD projector relies on a refresh of projected light, the imaging system with the DMD projector is faster than that with the mechanical platform. Nowadays, DMD is an important part of the design of LAPS systems. For example, a light-addressing device combining optical choppers with DMD has a 120 Hz refresh rate, which is the light source for LAPS and light-actuated AC electroosmosis integrated in an acting and sensing system.[53] Besides that of DMD projector, there is reported that the commercially available projector based on liquid crystal has been developed successfully for LAPS addressing.[54] The display based on an OLED or LCD consists of many luminous units arranged in a regular pattern, where each luminous unit of the displays can be turned on or

https://doi.org/10.1021/acsomega.3c04789
ACS Omega 2023, 8, 42028−42044

off independently through driven circuits. It can be found that the display based on an OLED or LCD is a prime light source for rapid imaging because it can shift the position of illumination without physical displacement of the illumination device, which is similar to the DMD projector. Werner et al has proposed a LAPS system with OLED display as light source,[55,56] where the imaging speed of OLED-LAPS using OLED display with high refresh rate can reach to 25 ms/spot.[56] Differing from switching mirrors, ref 52 mentioned another addressing method through modifying the refraction angle of a micromirror. However, the method about the refraction angle is not fit for the DMD projector. It is worth mentioning that this method is adopted by Das et al.[57,58] As shown in Figure 3b, an analog micromirror is controlled by a MEMS controller card to modify the refraction angle about the light beam from the red laser. The LAPS imaging system integrated with an analog micromirror can provide high-speed imaging with an imaging speed of 0.2 ms/spot.[58] With a similar method, Zhou et al. design a photoelectrochemical imaging system based on LAPS for rapid pH monitoring, where the high temporal resolution is credited to application of analog micromirror.[48]

2.1.2. Optimization of LAPS Imaging System with Lighting Array. It is clear that LAPS systems introduced in Section 2.1.1 implement imaging relying on a single light source. Although we can improve the imaging speed of a LAPS system by optimizing the light source,[52−58] the imaging mechanism of a single light source system which is obtaining pixels one by one is the possible reason to limit enhancement of spatial resolution for LAPS imaging. On the other hand, LAPS based on a single light source is not an ideal imaging device for monitors because each pixel in the chemical image is measured nonsimultaneously. Therefore, another type of LAPS system using a lighting array as an illumination device is proposed which can measure multiple pixels at the same time.[59−63] As shown in eq 2, there is $n_{measure} > 1$ for the LAPS system using a lighting array instead of a single light source. To employ the advantage of the lighting array, Wagner et al. propose the LAPS imaging system combining a linear stage and a vertical-cavity surface-emitting laser (VCSEL) array, where the VCSEL array supports high-density imaging and the linear stage is useful for increasing the illumination range and flexibility of imaging.[59] Figure 3c provides the schematic and picture of LAPS with a combined light source.

Because each illumination unit in the lighting array is modulated with an alternating current with a specific frequency, enhancement of the frequency bandwidth for the LAPS means a higher imaging speed because the frequency bandwidth decides the number of illumination units that can be integrated in the lighting array to excite the sensor. It has been proven that there are photocarriers generated and separated within the depletion region directly during front-side illumination.[60] Therefore, the LAPS system based on front-side illumination supports a wider frequency bandwidth compared with the LAPS system based on back-side illumination because of non-involving diffusion processes in the depletion region. As shown in Figure 3d, Itabashi et al. design a front-side-illuminated LAPS with LED array for pH monitoring, where the highest speed of imaging is 0.4 ms/spot and the LED array includes 7 × 5 LEDs.[61] Usually, the single core size of the multicore optical fibers is smaller than that of LED. Therefore, a lighting array based on multicore fibers can provide good spatial resolution and measurement speed for LAPS simultaneously, which is suitable for imaging in vivo of LAPS.[62] However, the signal-to-noise ratio of fiber-based LAPS should be improved, because the brightness of the fiber is weak. Generally, LAPS with front-side illumination requires a light source with lower brightness than that with back-side illumination. Miyamoto et al. design the chemical imaging system with high imaging speed for microfluidic channel monitoring.[63] Front-side illumination with optical fibers can provide an imaging speed up to 0.15 ms/spot.

Besides illumination of the front side, the frequency bandwidth of LAPS can be enhanced through optimizing the structure and the material of the substrate.[65−67] Truong et al. propose that the partially etched structure on a substrate can enhance the frequency bandwidth of LAPS.[65] p−i−n amorphous silicon (a-Si) and indium gallium zinc oxide (IGZO) are reliable semiconductors for LAPS, which have been proven by Yang et al.[66,67] The frequency stability of the spatial resolution (1−20 kHz) is confirmed in p−i−n a-Si LAPS.[66] Compared with LAPS based on Si substrate, IGZO LAPS supports a higher maximum frequency of light excitation (30 kHz).[67] Characteristics of LAPS with optimizing the imaging speed are summarized in Table 2.

2.2. Application of LAPS for Biochemistry Monitoring. One of the applications of the rapid imaging system based on LAPS is biochemistry monitoring.[51,68−70] The development of biological monitoring capabilities for LAPS is closely related to the improvement of the LAPS imaging speed. Early LAPS cost tens of minutes to form a chemical image with the help of mechanical platform addressing.[51] For example, Nakao et al. observe the growth of microorganism colonies with an early LAPS imaging system, where the time span for observation is in hours.[68]

Most monitoring examples are based on the principle of pH sensing.[39,69,70] Hiraishi et al. monitor pH distribution on the surface of bovine dentin using a LAPS imaging system.[69] LAPS imaging can be used to study crevice corrosion on stainless steel.[70−72] Miyamoto et al. design a LAPS system for in situ pH imaging in the vicinity of a corroding metal surface, which is shown in Figure 4a.[70] LAPS is an ideal method for indirectly observing the crevice corrosion because of the advantages of LAPS in pH imaging, where the change in pH will appear in the corrosion position. Subsequently, the new technology combining LAPS and infrared reflection technology is developed to support in situ imaging about pH and surface roughening simultaneously.[72] This indirect detection method[70−72] can also be applied for study hydrogen permeation,[73] where a pH change will appear in the anode surface of the iron sheet because of redox reaction.

LAPS can be applied to study the cell growth and metabolism. The imaging system addressing with a single light source and mechanical platform is applied for monitoring the recovery process of defects in a cultured cell layer.[46] Figure 4b shows the chemical images of the defect recovery process in the Caco-2 cell layer from day 1 to day 16. Dantism et al. studies the extracellular acidification of *Escherichia coli* (*E. coli*) K12 bacteria and CHO cells through differential imaging with the help of differential LAPS, where the time interval for imaging is 20 min.[39] The example in ref 39 proves that LAPS and ISFET have the same advantage, which is suitable for long-term measurements of extracellular acidification.[74]

LAPS can also be used to monitor enzymatic reaction.[33,34] Figure 4c shows an example of observation of a thin poly(ester amide) film degraded by the enzyme α-chymotrypsin.[33] As

https://doi.org/10.1021/acsomega.3c04789
ACS Omega 2023, 8, 42028−42044

Table 2. Characteristics of LAPS with Optimizing Imaging Speed

Year	Illumination displacement technology	Measurement area (mm^2)	Image size (spots)	Speed (ms/spot)	Measurement target	Light source	Ref
1994	X−Y stage	6 × 6	128 × 128	110	pH gradient between acid and base, pH image of yeast colonies cultured on an agar medium	He−Ne laser (λ = 633 nm) of 10 mW	51
2010	Refreshing of OLED display	NA	96 × 64	1000	pH image	Illuminated pixels of OLED display	55
2011	Combing the VCSEL array with linear stage	3 × 10	12 × 22	14	pH image with pattern	Miniaturized VCSEL array (λ = 850 nm) with maximum power = 2 mW	59
2011	Controlling of the OLED display by the driving circuit with high modulation frequencies	20.1 × 13.2	96 × 64	25	pH image with pattern	Illuminated pixels of OLED display	56
2012	DMD chip controlled with digital light processing (DLP)	20.8 × 15.6	8 × 6	41	pH image with pattern	Inner light source of the DLP system (Pico V2 development kit)	52
2013	Reflecting of analog micromirror	3.2 × 6.12	14 × 121	1	pH image with pattern	A laser (λ = 658 nm)	57
2013	LED matrix with 7 × 5 LEDs controlled by frequency division multiplex (FDM)	12.7 × 17.8	5 × 7	0.4	pH image	LED matrix with 7 × 5 LEDs, each LED unit with λ = 660 nm and illumination is 24 mcd	61
2014	Illumination array including 64 LEDs with optical fibers	12 × 12	8 × 8	0.15	pH image	Illumination array including 64 LEDs (λ = 600−625 nm and illumination intensity is 12500 mcd)	63
2014	Reflecting of analog micromirror	14.5 × 10.5	500 × 400	0.2	pH image with pattern	Red laser	58
2021	Reflecting of analog micromirror	0.16 × 0.16	20 × 20	0.3	pH image	Laser (λ = 405 nm) with 50 mW	48

shown in Figure 4d, Zhao et al. fix urease on the sensor plate and dynamically monitor the enzymatic reaction with urea-sensitive LAPS.[34]

In recent years, the combination of LAPS and microfluidic technology has been an important research direction.[63,64] As mentioned previously,[63] the rapid imaging system with imaging speed up to 0.15 ms/spot is used by Miyamoto et al. to view the buffering action inside a microfluidic channel at 100 fps, of which the scheme of the imaging system and pH images are displayed in Figure 4e.

Miniaturization of sensors is an important requirement for in vivo labeling experiments. Guo et al. develop a miniaturized LAPS system as a label-free pH probe placed inside the living body.[75] As shown in Figure 4f, in vivo label-free pH probes combining LAPS and multimodal fibers can provide pH acquisition in real time at multiple pixels simultaneously. The pH probe based on LAPS catches successfully the local pH changes in the hippocampus of rats caused by pinch toe stimulation.

In this section, the technologies about enhancing the imaging speed with a single light source and lighting array are analyzed. Multiple applications such as monitoring metal corrosion,[70−72] observing cell layer recovery,[46] etc., have demonstrated the monitoring ability of the LAPS imaging systems. LAPS supports multiple research objectives, including microorganism colonies,[68] bovine dentin,[69] metal surfaces,[70−72] cells,[39,46] etc. At present, most examples are based on pH detection mechanisms. More biochemical monitoring systems based on other detection mechanisms, such as enzymatic reaction,[33,34] DNA detection, etc., need to be developed. It can be expected that more ideas, such as a more cost-efficient light source for a rapid LAPS system, miniaturization of LAPS,[1,75] etc., will be proposed to improve the application value of a rapid imaging system based on LAPS. On the other hand, through the example about crevice corrosion imaging,[70−72] we can know that LAPS imaging systems are developing toward integration. By combining LAPS with different detection technologies, such as infrared reflection technology,[72] microfluidic technology,[63,64] etc., the new sensor platform can undertake more complex tasks.

3. TECHNOLOGY OF HIGH-RESOLUTION IMAGING FOR LAPS

3.1. Improvement of Spatial Resolution. Besides imaging speed, another essential target for the LAPS imaging system is spatial resolution. Normally, there are several distances to represent spatial resolution obtained through scanning LAPS with stripe pattern, such as the length from the illumination position with high photocurrent to that with photocurrent decayed to e^{-1},[76,77] the minimum resolved diameter of the pattern covering the substrate surface,[78] the length from the illumination position with 40% maximum normalized photocurrent to that with 60% normalized photocurrent,[65,79,80] the full width at half-maximum (fwhm) value of photocurrent curve of the first derivation,[81] etc.

We cannot investigate spatial resolution without consideration of the lateral diffusion of photocarriers appearing inside the substrate. According to the theory research, not only the doping concentration of substrate but also the thickness of the semiconductor will affect the lateral diffusion of photocarriers of LAPS.[82,83] The distance of lateral diffusion $Y_{lateral}$ which represents the length from the illumination position to the

https://doi.org/10.1021/acsomega.3c04789
ACS Omega 2023, 8, 42028−42044

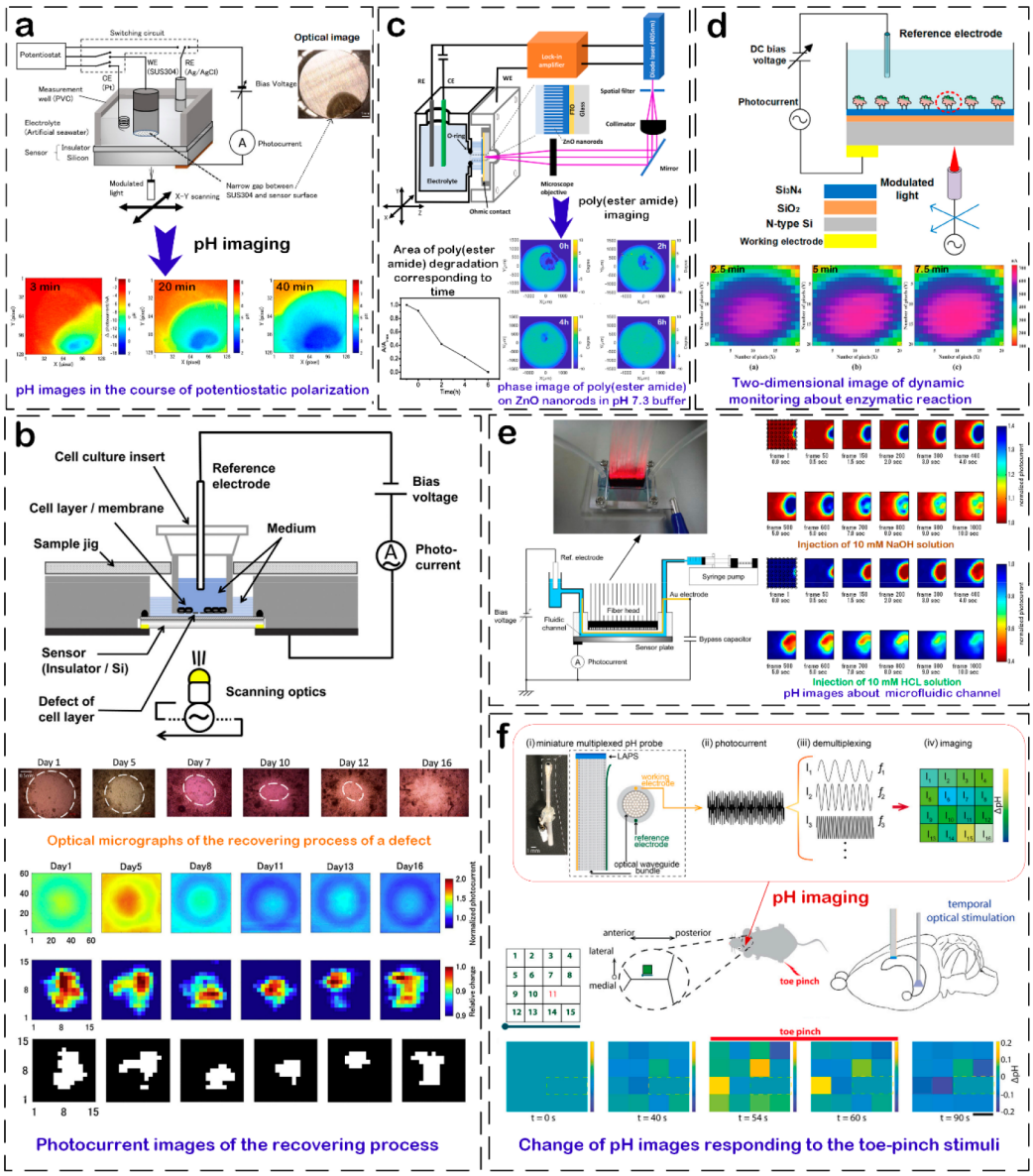

Figure 4. Application and related technology of LAPS for biochemistry monitoring. (a) In situ pH imaging in the vicinity of a corroding metal surface. Reproduced with permission from ref 70. Copyright 2015 Elsevier. (b) Visualization of the recovery process of defects in a cultured cell layer. Reproduced with permission from ref 46. Copyright 2016 Elsevier. (c) Monitoring the degradation of a thin poly(ester amide) film with the enzyme α-chymotrypsin. Reproduced with permission from ref 33. Copyright 2018 American Chemical Society. (d) Dynamic monitoring of enzymatic reactions. Reproduced with permission from ref 34. Copyright 2022 Elsevier. (e) Visualization of buffering action inside the microfluidic channel. Reproduced with permission from ref 63. Copyright 2014 Elsevier. (f) Real-time in vivo multiplexed pH acquisition. Reproduced with permission from ref 75. Copyright 2020 Elsevier.

position with minority carriers decayed to e^{-1} can be described as[82]

$$Y_{lateral} = \sqrt{L_p(L_p+2d)} \quad (3)$$

where L_p is the diffusion length of minority carriers inside substrate, d is the thickness of substrate. The smaller the $Y_{lateral}$, the faster the decay speed of the number of minority carriers, which means that a higher spatial resolution of LAPS can be obtained. Therefore, it is obvious that there are two strategies for optimization of spatial resolution directly. One is to reduce the thickness d, and the other is to choose the substrate with small L_p.

3.1.1. Thickness Reduction of Silicon Substrates. The n-doped or p-doped silicon (monocrystalline and polycrystalline silicon) with a thickness of 100−400 μm is a prevailing material of the LAPS substrate because of cost and fabrication, where the spatial resolution of corresponding LAPS is 100−500 μm. Similarly, there are many theoretical research works about spatial resolution using Si LAPS as the object.[82,84,85] In this section, we will introduce thickness reduction technology based on silicon substrates for improving spatial resolution.

The thin substrate can be obtained through decreasing the thickness of the thick Si wafer with physical or chemical method, such as wet etching,[86−88] ion etching,[89,90] etc. Nakao et al. etch n-type Si with KOH to optimize LAPS, where the spatial resolution is improved to 10 μm by etching the n-type Si wafer with hundreds of micrometers thickness to 20 μm.[86] However, LAPS with a thin Si layer as substrate is difficult to

https://doi.org/10.1021/acsomega.3c04789
ACS Omega 2023, 8, 42028−42044

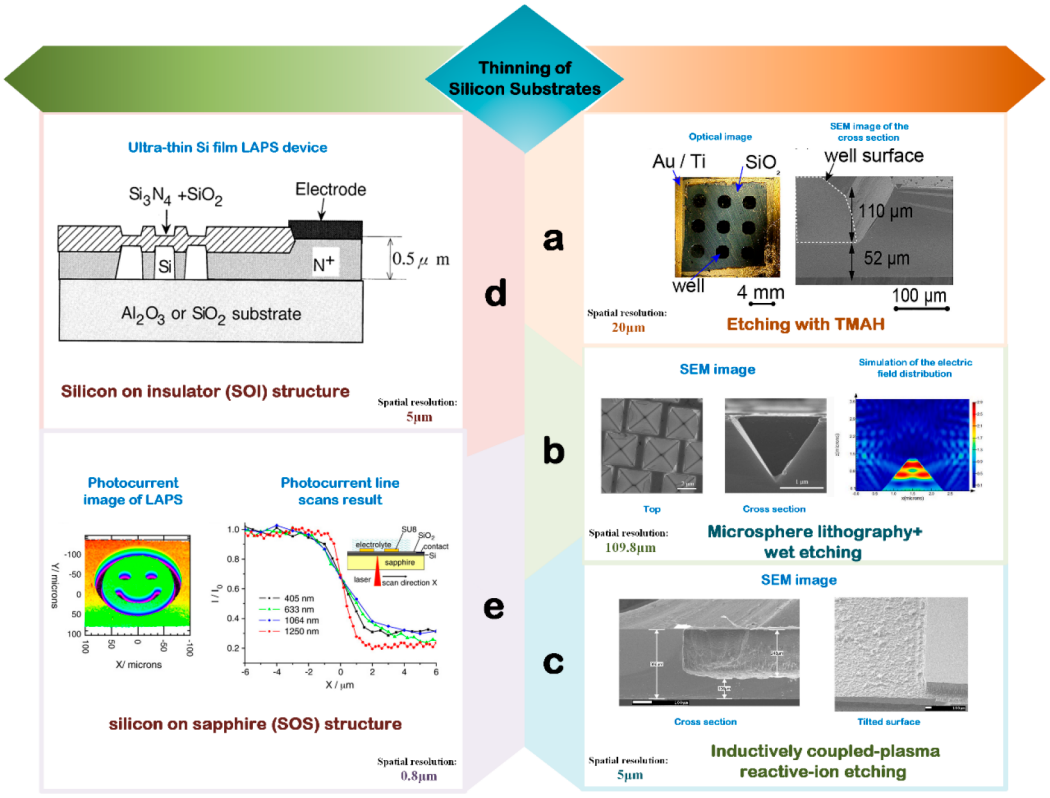

Figure 5. Typical designs applied to thin Si LAPS. (a) Multiwell structure partially etched with TMAH. Reproduced with permission from ref 88. Copyright 2019 John Wiley and Sons. (b) Well-ordered pyramidal pits-patterned silicon for LAPS. Reproduced with permission from ref 79. Copyright 2022 Elsevier. (c) Thickness decreasing of Si substrate through etching with the help of ICP-RIE. Reproduced with permission from ref 89. Copyright 2017 Elsevier. (d) Ultrathin Si LAPS based on SOI structure. Reproduced with permission from ref 78. Copyright 1998 Elsevier. (e) LAPS based on SOS structure. Reproduced with permission from ref 76. Copyright 2010 Elsevier.

apply in practice because of a lack of mechanical strength. To solve this problem, LAPS with a local thinning substrate is proposed. Chen et al. construct the structure of 100 μm deep blind holes on Si wafer with 300 μm thickness through silicon anisotropic wet etching,[87] where the performance of LAPS is improved and the mechanical strength is maintained because of a local thinning substrate. Truong proposes a type of LAPS with partially etched structure, where the Si substrate is thinned with tetramethylammonium hydroxide (TMAH).[65] In partially etched LAPS, the thicknesses of the etched region and frame region are 47 and 150 μm, respectively. Compared with the 40 μm achieved in the frame region, spatial resolution measured in the etched region is improved to 20 μm. In subsequent research, LAPS with a multiwell sensor platform based on the same etching technology as that in ref 65 is designed.[88] As shown in Figure 5a, there are several etching wells with a depth of 100 μm as the measuring region in a sensor plate. The spatial resolution for LAPS with the multiwell sensor platform is less than 20 μm, which is based on the premise that the thickness of LAPS in the etching well is 47 μm. Recently, we have proposed the LAPS using well-ordered pyramidal pits-patterned silicon as the substrate.[79] As shown in Figure 5b, the structure of a well-ordered pyramidal pits-pattern on the substrate is fabricated by microsphere lithography and wet etching, where the microsphere lithography technology decides the shape of etching wells and wet etching is based on KOH solution. Because the etching wells on the illumination area of LAPS can increase the signal-to-noise ratio by reducing light reflection, LAPS with well-ordered pyramidal pits-patterned silicon can provide nearly twice the spatial resolution improvement compared with LAPS based on flat silicon. Instead of wet etching technology, Yang et al. decrease the Si substrate by inductively coupled-plasma reactive-ion etching (ICP-RIE),[89] which can not only optimize the spatial resolution but also increase the photocurrent by processing substrate with ICP-RIE. As shown in Figure 5c, LAPS with a thickness of 100 μm provides spatial resolution of 5 μm for 2D chemical imaging, which is not inferior to that of LAPS introduced in ref 86. Zeng et al. use deep reactive-ion etching (DRIC) technology to reduce the thickness of Si wafer from 350 to 100 μm.[90] As it turns out, thinning the Si substrate of LAPS by DRIC can improve the performance of photocurrent and spatial resolution, in which the photocurrent increased by three times compared with non-etched LAPS, and the spatial resolution of etched LAPS is 100 μm.

Silicon on insulator (SOI)[78] and silicon on sapphire (SOS)[76,91] are two types of structures with an ultrathin Si layer and used to fabricate LAPS devices. As shown in Figure 5d, Ito designs ultrathin Si film LAPS[78] based on SOI, where the thickness of the Si layer is 0.5 μm. Thanks to the ultrathin Si layer, the spatial resolution of SOI-base LAPS is less than 5 μm. Figure 5e shows a high-resolution LAPS with SOS substrate.[76] In another instance, the thickness of the Si layer in SOI is 1 μm, and it is proved that the spatial resolution of LAPS is less than 1 μm in combination with a specific illumination method.[91] LAPS based on SOI or SOS has a brilliant imaging performance. We look forward to reducing

https://doi.org/10.1021/acsomega.3c04789
ACS Omega 2023, 8, 42028−42044

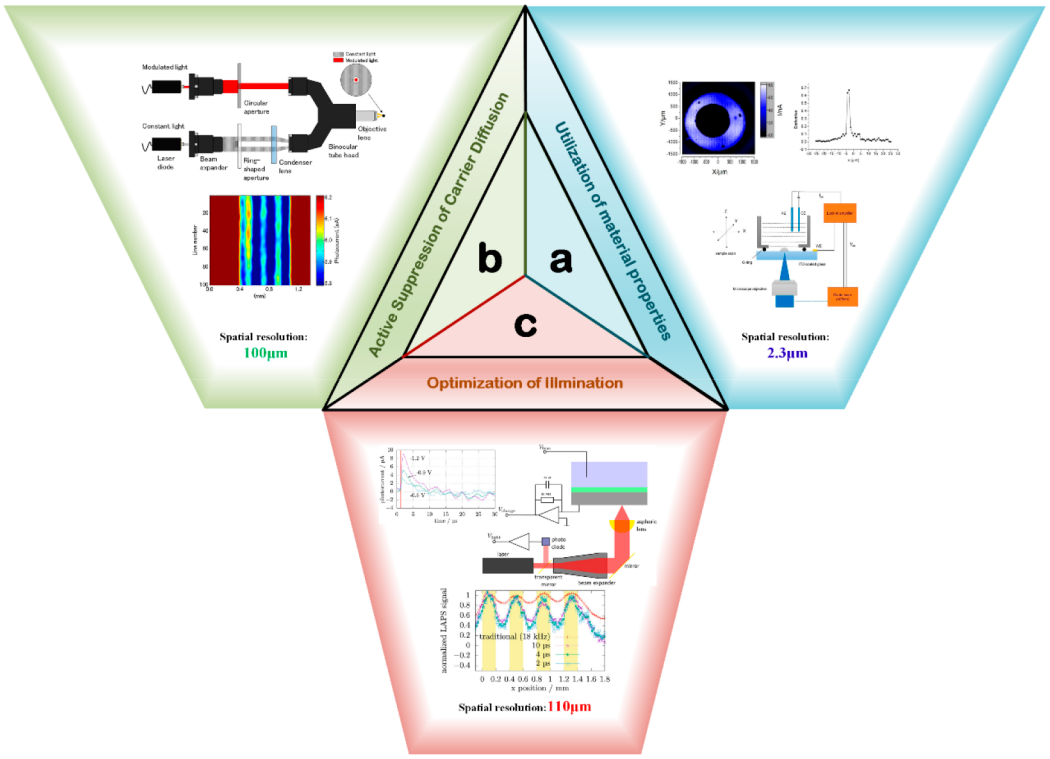

Figure 6. Typical example of improving spatial resolution by utilization of material properties. Active suppression of carrier diffusion and optimization of illumination. (a) Scheme and imaging result of LAPS using ITO glass as substrate for imaging. Reproduced with permission from ref 45. Copyright 2017 American Chemical Society. (b) Illumination scheme and imaging result of LAPS with a hybrid illumination. Reproduced with permission from ref 102. Copyright 2018 Elsevier. (c) Scheme and spatial resolution result of pulse-driven light-addressable potentiometric sensor. Reproduced with permission from ref 103. Copyright 2017 Elsevier.

the cost of SOI and SOS with the development of a material process in the future.

3.1.2. Utilization of Material Properties. The spatial resolution of LAPS can be improved by utilizing a semiconductor with a low diffusion length, because the phenomenon of lateral diffusion about photocarriers is related to the diffusion length. There are many semiconductors with low diffusion, such as AsGa,[92] amorphous silicon,[93,94] etc., that have been used in fabrication of LAPS. Das et al. propose LAPS with a-Si as a semiconductor layer, in which the thickness and diffusion length of the semiconductor layer are 1 and 0.57 μm, respectively. There is a high spatial resolution of 25 μm for a-Si LAPS with illumination of a miniprojector.[94] Tu et al. propose LAPS with a simple structure and high spatial resolution (2.3 μm) because ZnO nanorods synthesized on FTO-coated glass are used to construct a semiconductor without the traditional sensing membrane and insulator layer of LAPS.[33] The 1D ZnO nanorods-based LAPS has good spatial resolution because the diameter of 1D ZnO nanorods is less than 80 nm and the light scattering effect is negligible. Recently, Li et al. have proposed bipolar LAPS based on a fullerene layer with excellent pH sensitivity (150 mV/pH) and high spatial resolution (3.8 μm), which is owed to the small diffusion length (≈40 nm) and small thickness of the semiconductor layer (5 μm).[95] As a commercially transparent electrode, indium−tin oxide (ITO) glass is used as the substrate by Zhang et al. for LAPS fabrication.[45] As shown in Figure 6a, the thin ITO layer plays the roles of electrode, semiconductor, and sensing membrane of LAPS. Compared with Si, ITO is a low cost and robust material for LAPS design. Combining with a light source with a specific wavelength (405 nm), LAPS based on commercial ITO glass can provide high spatial resolution imaging (2.3 μm). Similar to ITO, IGZO is another material of transparent electrode which has been used as the semiconductor material of LAPS. Yang et al. design and optimize the IGZO LAPS, which achieves a spatial resolution less than 50 μm.[96]

LAPS with a multilayer semiconductor is the novel target for fabrication of LAPS.[66,97,98] Zhou et al. design a LAPS with a stacked structure of the semiconductor including the GaN layer and InGaN layer to increase the spatial resolution, which is up to 7 μm.[97] LAPS with an InGaN/GaN layer can be applied for cell imaging. Yang et al. design a thin-film LAPS with p−i−n amorphous silicon as the semiconductor layer.[66,98] Compared with a-Si LAPS, the photovoltage of LAPS with p−i−n amorphous silicon is increased by 50% because the p−i−n amorphous structure can provide good photoelectric transmission efficiency and a conductive path for the photocarrier inside the LAPS. Importantly, frequency stability is investigated in LAPS with p−i−n amorphous silicon.

3.1.3. Active Suppression of Carrier Diffusion. The strategies introduced in Sections 3.1.1 and 3.1.2 reduce carrier diffusion in a passive approach. In this section, we will present the strategy about active suppression of carrier diffusion.

Guo et al. propose the LAPS with a combined light source which consists of an alternating-modulated light beam and a ring of constant illumination surrounding it.[99,100] The constant illumination provides photocarriers that limit the lateral diffusion of carriers from the alternating-modulated light by enhancing the composite. The novel illumination method proved that it can improve spatial resolution of LAPS through device simulation. Afterward Ko-ichiro Miyamoto verifies the

https://doi.org/10.1021/acsomega.3c04789
ACS Omega 2023, 8, 42028−42044

feasibility of combined light source by experiment, where two types of hybrid illumination, illumination based on a bundle of optical fibers[101,102] and based on a binocular tube head,[102] are designed. As shown in Figure 6b, The LAPS system with a 200 μm thick Si substrate and hybrid illumination based on a binocular tube head can image with spatial resolution less than 100 μm.[102]

Recently, we have designed the LAPS with a honeycomb meshed working electrodes, which can reduce the lateral diffusion of carrier because the light beam will be separated into several sublights for a small lateral diffusion length and the carrier concentration in the honeycomb hole is much higher than that in the adjacent metal boundary.[80] Therefore, LAPS with honeycomb meshed working electrodes has a higher spatial resolution compared with LAPS with flat working electrodes.

3.1.4. Optimization of Illumination. According to the principle of LAPS,[13] illumination will excite the photocarriers within the semiconductor, which leads to the appearance of photocurrent. The factors of light source, such as the diameter of light beam, frequency, and wavelength of alternating-modulated illumination, etc., will affect the spatial resolution directly. As mentioned in Section 3.1.1 pyrimidal pits-pattern on the silicon changes the route of light beam and makes the illumination focus on detection position.[79] The surface design will lead to improvement of the spatial solution because of optimization of illumination. Werner proved that it is useful to optimize the excitation method for high spatial resolution. The pulse-driven LAPS is shown in Figure 6c, in which the pulse with the length of 300 ns is used to drive the illumination.[103] Compared with the excitation method of continuous modulation, the higher spatial resolution can be observed by reading out the integrated photocurrent within the short time after illumination because the lateral diffusion will occur after illumination, which is the main reason for lateral diffusion. Therefore, integration of the photocurrent can lead to a lower lateral diffusion and, furthermore, higher spatial resolution.

Theoretically, the bigger wavelength of light sources will cause the deeper penetration of illumination into the Si substrate, where the higher spatial resolution can be obtained.[82] Wang et al. verify another conclusion in SOS LAPS modified with an octadecyl monolayer since the focus of the light source is dependent on wavelength.[77] LAPS based on the IGZO substrate[96] displays excellent spatial resolution by modification of the wavelength and duty cycle of illumination modulated with a square wave. In tradition, although we look forward to the higher wavelength of illumination, which means a higher penetration depth and brings a higher spatial resolution, the bandgap of the materials limits the wavelength of illumination. Chen et al. use the laser with lower energy than silicon (wavelength = 1250 nm) to break out the limitation and excites SOS LAPS successfully because of the application of a two-photon effect.[76]

One of the direct methods to improve spatial resolution is utilization of a light beam with a small diameter. LAPS based on AsGa introduced in ref 92 provides a high spatial resolution because of the substrate material and light beam based on a CD-ROM with a small diameter (2.6 μm). Besides, many types of light source, such as a miniprojector,[52] OLED display,[55,56] analog micromirror,[58] VCSEL,[59] etc., have been verified as reliable light sources for high-resolution LAPS because of their unique advantages, respectively.

Alternating-modulated illumination plays the role of excitation of the carriers within the substrate. However, exciting LAPS with illumination is not a unique option. An ion sensor using electron beam but not light beam to excite LAPS plate is proposed.[81,104] This sensor, named electron-beam-addressable potentiometric sensor (EAPS), has a detection mechanism similar to that of LAPS and is observed to provide sub-micrometer level ion imaging. Nii et al. design EAPS with spatial resolution in sub-micrometer level (216 nm) by applying the electron beam for SOI LAPS with 50 nm thick Si,[81] which indicates that the potential of biochemical sensing systems is based on the LAPS mechanism. Table 3 lists the technical features of LAPS with optimizing spatial resolution which are mentioned in Section 3.1.

3.2. Application of High-Resolution LAPS for Biochemical Imaging. High spatial resolution allows LAPS to be applied for the study of microbiology, such as cell imaging,[13] colony imaging,[86] etc. In 1990s, LAPS has been used for *Escherichia coli* (*E. coli*) colonies imaging through pH response.[86] As mentioned above, LAPS has been used for imaging a cultured cell layer.[46] Dantism et al. analyze the relationship between metabolic activity and extracellular acidification about *E. coli* K12 and Chinese hamster ovary (CHO) cells by differential LAPS imaging.[39] Zhang et al. obtain the chemical image about multilayer yeast *Saccharomyces cerevisiae* by SOS LAPS.[105] Obviously, the clear image that is shown in Figure 7a relies on SOS LAPS with high spatial solution. However, due to contact problem, the image of an individual cell cannot be obtained in ref 105. Furthermore, Jacques et al. design a photoelectrochemical imaging system (PEI) integrating SOS LAPS,[106] which improves the contact between cells and sensor surfaces by applying pressure to the organoid. PEI can clearly obtain images with two cardiomyocyte cells.

Recently, LAPS has been reported to be utilized for individual imaging. For example. Zhou et al. design the photoelectrochemical imaging system based on SOS LAPS for B50 cells imaging, where the single cell contour can be distinguished in the photocurrent image.[48] As shown in Figure 7b, the chemical image about single mesenchymal stem cell is obtained by LAPS with high spatial resolution (7 μm), which has the semiconductor of an InGaN/GaN layer.[97]

Chemical reaction, such as enzymatic reaction[33,34] and electrochemical reaction,[70,107] is an important branch of LAPS application. LAPS is often used to study chemical imaging. For example, LAPS based on a ZnO nanorod substrate is used to image the degradation process of a thin polyfilm with the enzyme α-chymotrypsin.[33] LAPS can also be applied to electrochemical reaction imaging. As shown in Figure 7c, Chen et al. observe water electrolysis through LAPS, in which the size of the measurement area is 2 μm × 2 μm per pixel.[107]

Accurate control of the injected solution is crucial in microfluidic technology. LAPS can provide an efficient, accurate, and pollution-free observation for microinterfaces within channels. Figure 7d displays the chemical images of the laminar flows in a Y-shaped microchannel with the width of 160 μm.[108] Besides, LAPS imaging system can be used for high-speed chemical imaging inside a microfluidic channel[63] and observation of enzymatic reaction in the microfluidic channel.[109,110] For example, Welden et al. build an observation and regulation system for pH gradient changes in microfluidic channels, where LAPS is applied to study the pH changes

https://doi.org/10.1021/acsomega.3c04789
ACS Omega 2023, 8, 42028−42044

Table 3. Characteristics of LAPS with Optimizing Spatial Resolution

Year	Technology characteristic	Substrate	Illumination source	Spatial resolution	Optimization type	Ref
1996	Thinning the substrate and using infrared laser as the light source	20 μm thick n-type Si substrate	Semiconductor infrared laser (λ = 830 nm)	10 μm	Thickness reduction of silicon substrates	86
1998	Silicon on insulator (SOI)	0.5 μm thick n-type polycrystalline Si substrate made on quartz substrate	Green laser with 3 mW (λ = 532 nm, focus of 1.8 mm)	5 μm	Thickness reduction of silicon substrates	78
2000	GaAs as substrate, a miniaturized light source based on a CD-ROM player	8 μm thick GaAs	CD-ROM optic with 180 μW (λ = 780 nm, focus of 2.6 μm)	3 μm	Utilization of material properties; optimization of illumination	92
2000	Decreasing the thickness of low doping substrate	3 μm thick n-type Si substrate	Semiconductor laser diode with 10 mW (λ = 690 nm)	15 μm	Thickness reduction of silicon substrates, utilization of material properties	85
2004	Thin amorphous silicon layer on transparent glass as substrate	Amorphous silicon layer with thickness of 0.3−1.5 μm	Optics of DVD drive	1 μm	Utilization of material properties; optimization of illumination	93
2006	Silicon on sapphire	1 μm thick p-type silicon layer on 475 μm thick sapphire substrate	He−Ne laser with 5 mW (λ = 632 nm)	1 μm	Thickness reduction of silicon substrates	91
2010	Silicon on sapphire; using two-photon effect on silicon to generate the photocurrent	0.5 μm thick p-type Si on 500 μm thick sapphire	Femtosecond Cr−forsterite laser with 200 mW (λ = 1250 nm)	0.8 μm	Thickness reduction of silicon substrates; optimization of illumination	76
2011	OLED display providing illumination	N-type Si	OLED display (illumination spot size = 400 μm × 200 μm)	200 μm	Optimization of illumination	56
2014	Thin amorphous silicon layer on ITO glass; commercial DLP-based video projector using as light source	Amorphous Si layer with thickness of 1 μm	DLP-based video projector combining with 4× projection lens (smallest size of light spot = 72 μm × 72 μm)	25 μm	Utilization of material properties; optimization of illumination	94
2015	Silicon on sapphire; choosing the light source with suitable wavelength	0.5 μm thick p-type Si on 475 μm thick sapphire substrate	Laser with wavelength of 405 nm	1.6 μm	Thickness reduction of silicon substrates; optimization of illumination	77
2016	Growing P−I−N amorphous Si on ITO/glass	12 nm thick p-type a-Si + 100 nm thick i-type a-Si + 20 nm thick n-type a-Si	Red laser with wavelength of 658 nm	115 μm (illumination frequencies = 1, 10, and 20 kHz)	Utilization of material properties	66
2017	Utilizing high-frequency pulse as light excitation (illumination frequency ≈ 3.33 MHz)	200 μm thick n-type Si	Diode laser with focus system (λ = 905 nm, diameter of light beam = 1.1 μm, maximum power = 85 mW)	110 μm	Optimization of illumination	103
2017	Thinning the substrate by deep reactive-ion etching	100 μm thick p-type Si substrate	Red laser	100 μm	Thickness reduction of silicon substrates	90
2017	Indium tin oxide (ITO)-coated glass as substrate	ITO-coated glass (50 Ω/cm^2)	Diode laser with 50 mW (405 nm, illumination spot diameter ≈ 1 μm)	2.3 μm	Utilization of material properties	45
2018	1D ZnO nanorod arrays synthesized on FTO-coated glass as substrate	4.03 ± 0.025 μm	Diode laser with 50 mW (λ = 405 nm, focused spot diameter ≈ 1 μm)	3 μm	Utilization of material properties	33
2018	Hybrid illumination based on a binocular tube optics	200 μm thick n-type Si	Hybrid illumination system utilizing a binocular tube head and two laser diodes (λ = 832 nm)	100 μm	Active suppression of carrier diffusion	102
2018	Partially thinning the substrate by anisotropic etching process based on tetramethylammonium hydroxide	Etched region of n-type Si with thickness of 47 μm	Laser with wavelength of 830 nm	20 μm	Thickness reduction of silicon substrates	65, 88
2018	Thinning the substrate by inductively coupled plasma reactive-ion etching	p-type Si substrate with thickness of 100 μm	Red laser (λ = 658 nm)	5 μm	Thickness reduction of silicon substrates	89
2019	Semiconductor layer composed of InGaN and GaN growing on sapphire substrate	100 nm thick InGaN + 40 nm thick GaN	Diode laser with 50 mW (λ = 405 nm)	7 μm	Utilization of material properties	97
2021	Sensors with honeycomb meshed working electrodes	100 μm thick n-type Si substrate with honeycomb meshed working electrodes	Diode laser (λ = 638 nm, m diameter of light bea= 30 μm)	120 μm	Active suppression of carrier diffusion; optimization of illumination	80

https://doi.org/10.1021/acsomega.3c04789
ACS Omega 2023, 8, 42028−42044

Table 3. continued

Year	Technology characteristic	Substrate	Illumination source	Spatial resolution	Optimization type	Ref
2021	Indium gallium zinc oxide (IGZO) on ITO glass as substrate	300 nm thick IGZO (In:Ga:Zn:O = 1:1:1:4; purity = 99.9%)	Laser in LED illumination systems with square wave modulated(λ = 405 nm, spot = 25 μm × 25 μm)	Less than 50 nm	Utilization of material properties; optimization of illumination	96
2021	Fullerene (C60) deposited on ITO as the semiconductor layer	60 nm thick C_{60}	Laser (λ = 405 nm, diameter ≈ 5 μm)	3.8 μm	Utilization of material properties	95
2023	Etching the well-ordered pyramidalpits-patterned in silicon substrate	thick n-type Si with thickness of 98−100 μm	Laser(λ = 650 nm)	109.8 μm	Thickness reduction of silicon substrates; optimization of illumination	79

caused by penicillin enzymatic reactions in a 1 mm wide microfluidic channel.[110]

In this section, we analyze the strategies about improving the spatial resolution and introduce them with examples. From the applications of high-resolution LAPS, it is obvious that the typical applications of high-resolution LAPS are unlabeled imaging of cell populations or even a single cell. The prerequisite for applying LAPS to single cell imaging is that its spatial resolution is less than 10 μm.[48,97,110] SOS LAPS seems to be very promising. In practical applications, the improvement of the imaging performance not only depends on spatial resolution[97,107] but also depends on the contact between the sample and the sensor surface,[109,110] where the former can be improved through strategies mentioned in Section 3.1 and the latter indicates the importance of appropriate sample fixation methods. Meanwhile, LAPS is an adaptable sensing technology for microfluidic systems, where it can serve as a reliable biochemical imaging technology for lab on chip systems based on its easy surface modification characteristics.[63,108−110] Recently, this strategy of integrating LAPS into microfluidic systems is applied to the low-temperature transport of cells, where the LAPS modified by elastic electrospun fibers plays an important role in protecting cells and accurately controlling the microenvironment.[111] We expect that more new application scenarios can be excavated for the microfluidic systems combined with LAPS, such as monitoring of the cell culture in the microchannel, component analysis of a trace sample, drug selection based on a trace sample, etc.

4. CONCLUSIONS

Hereby, we review recent studies about improving the chemical speed and spatial resolution, respectively. Imaging speed and the spatial resolution are two vital indicators for evaluating the performance of a biochemical imaging system using a microscale. However, the relationship between the two indicators is mutual restraint within a certain measuring range. When the increase of the pixel numbers improves the spatial resolution, the imaging speed will be reduced. Therefore, there is an important topic to find a balance between the imaging speed and the spatial resolution based on the requirement for different conditions.

With the development of biochemistry, the demand for microscale observation has grown urgent. The LAPS-based biochemical imaging system with rapid chemical speed has played an important role in the dynamic monitoring of the biochemical process, such as the corroding of a metal surface, the recovery process of defects in a cultured cell layer, the metabolism of bacteria and eukaryotic cells, enzymatic reactions, etc. And the system with high spatial resolution is adapted in the field that has the demand for detecting the object in the micrometer scale, for instance, the cellular observation. Reviewing the development history of the LAPS-based biochemical imaging system, we can find that the innovation of lighting devices and semiconductor materials will promote the development of this imaging system.

In further, there are several possible breakthroughs of microscale imaging of LAPS with the development of material and microelectronics technology, including the density of lighting arrays, the flexibility of an imaging mechanism, the application of advanced materials, such as monolayer two-dimensional materials, polymer materials, etc. Surely, the miniaturization and generality of the LAPS-based imaging

https://doi.org/10.1021/acsomega.3c04789
ACS Omega 2023, 8, 42028−42044

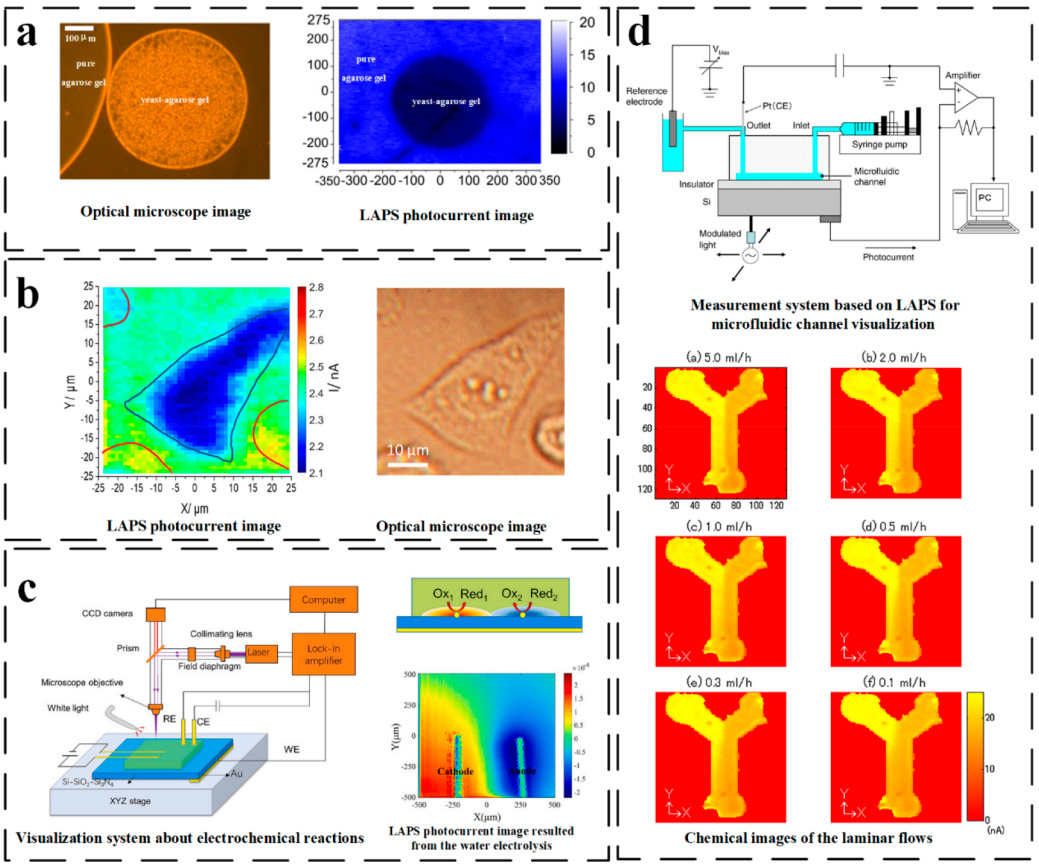

Figure 7. Examples and images of LAPS imaging for biochemical imaging on microscale. (a) LAPS imaging for the multilayer yeast *Saccharomyces cerevisiae* based on surface negative charge and the local impedance changing. Reproduced with permission from ref 105. Copyright 2016 Elsevier. (b) LAPS for single cell imaging, where the imaging target is a mesenchymal stem cell. Reproduced with permission from ref 97. Copyright 2019 The Authors under Creative Commons International Attribution License CC BY 4.0, published by MDPI. (c) Scheme of LAPS system and chemical image of water electrolysis. Reproduced with permission from ref 107. Copyright 2022 Elsevier. (d) Ion profile of laminar flows in a microfluidic channel. Reproduced with permission from ref 108. Copyright 2013 Elsevier.

system are also important, which are the key to serviced to business. We also look forward to when LAPS can participate in various complex detection platforms as a subunit.

AUTHOR INFORMATION

Corresponding Author

Shibin Liu − *School of Electronics and Information, Northwestern Polytechnical University, Xi'an, Shaanxi 710072, People's Republic of China;* orcid.org/0000-0003-3823-0162; Email: liushibin@nwpu.edu.cn

Authors

Jiezhang Luo − *School of Electronics and Information, Northwestern Polytechnical University, Xi'an, Shaanxi 710072, People's Republic of China*

Yinhao Chen − *School of Electronics and Information, Northwestern Polytechnical University, Xi'an, Shaanxi 710072, People's Republic of China*

Jie Tan − *School of Electrical Engineering and Electronic Information, Xihua University, Chengdou, Sichuan 610097, People's Republic of China*

Wenbo Zhao − *Institute of Flexible Electronics, Northwestern Polytechnical University, Xi'an, Shaanxi 710072, People's Republic of China*

Yun Zhang − *School of Electronics and Information, Northwestern Polytechnical University, Xi'an, Shaanxi 710072, People's Republic of China*

Guifang Li − *School of Electronics and Information, Northwestern Polytechnical University, Xi'an, Shaanxi 710072, People's Republic of China*

Yongqian Du − *School of Electronics and Information, Northwestern Polytechnical University, Xi'an, Shaanxi 710072, People's Republic of China*

Yaoxin Zheng − *Beijing Automation Control Equipment Institute, Beijing 100074, People's Republic of China*

Xueliang Li − *School of Mechanical and Electrical Engineering, Zhoukou Normal University, Zhoukou, Henan 466001, People's Republic of China*

Huijuan Li − *College of Electrical Engineering, Shaanxi Polytechnic Institute, Xianyang, Shaanxi 712000, People's Republic of China*

Yue Tan − *School of Electronics and Information, Northwestern Polytechnical University, Xi'an, Shaanxi 710072, People's Republic of China*

Complete contact information is available at: https://pubs.acs.org/10.1021/acsomega.3c04789

Notes

The authors declare no competing financial interest.

ACKNOWLEDGMENTS

This work is supported by the National Natural Science Foundation of China (Grant No. 61873209) and is partly

supported by the Fundamental Research Funds for the Science, Technology and Innovation Commission of Shenzhen Municipality (Grant No. JCYJ20180306171040865) and the Natural Science Basic Research Program of Shaanxi Province (Grant No. 2020JQ-206).

REFERENCES

(1) Grenier, V.; Walker, A. S.; Miller, E. W. A small-molecule photoactivatable optical sensor of transmembrane potential. *J. Am. Chem. Soc.* **2015**, *137*, 10894−10897.
(2) Bruggemann, D; Wolfrum, B; Maybeck, V; Mourzina, Y; Jansen, M; Offenhausser, A Nanostructured gold microelectrodes for extracellular recording from electrogenic cells. *Nanotechnology* **2011**, *22*, 265104.
(3) Akaike, N.; Harata, N. Nystatin perforated patch recording and its applications to analyses of intracellular mechanisms. *Jpn. J. Physiol.* **1994**, *44*, 433−473.
(4) Liu, X. W.; Yang, Y.; Wang, W.; Wang, S.; Gao, M.; Wu, J.; Tao, N. Plasmonic-based electrochemical impedance imaging of electrical activities in single cells. *Angew. Chem., Int. Ed.* **2017**, *56*, 8855−8859.
(5) Lu, J.; Li, J. Monitoring DNA conformation and charge regulations by plasmonic- based electrochemical impedance platform. *Electrochem. Commun.* **2014**, *45*, 5−8.
(6) Liang, W.; Wang, S.; Festa, F.; Wiktor, P.; Wang, W.; Magee, M.; LaBaer, J.; Tao, N. Measurement of small molecule binding kinetics on a protein microarray by plasmonic-based electrochemical impedance imaging. *Anal. Chem.* **2014**, *86*, 9860−9865.
(7) Martinoia, S.; Rosso, N.; Grattarola, M.; Lorenzelli, L.; Margesin, B.; Zen, M. Development of ISFET array-based microsystems for bioelectrochemical measurements of cell populations. *Biosens. Bioelectron.* **2001**, *16*, 1043−1050.
(8) Parak, W. J.; George, M.; Gaub, H. E.; Bohm, S.; Lorke, A. The field-effect- addressable potentiometric sensor/stimulator (FAPS) - a new concept for a surface potential sensor and stimulator with spatial resolution. *Sens. Actuators, B* **1999**, *58*, 497−504.
(9) Bohm, S; Parak, W.J; George, M; Gaub, H.E; Lorke, A Characterization of the field-effect addressable potentiometric sensor (FAPS). *Sens. Actuators, B* **2000**, *68*, 266−273.
(10) Karimi-Maleh, H.; Orooji, Y.; Karimi, F.; Alizadeh, M.; Baghayeri, M.; Rouhi, J.; Tajik, S.; Beitollahi, H. D.; Agarwal, S.; Gupta, V. K.; Rajendran, S.; Ayati, A.; Fu, L.; Sanati, A. L.; Tanhaei, B.; Sen, F.; Shabani-nooshabadi, M.; Asrami, P. N.; Al-Othman, A. A critical review on the use of potentiometric based biosensors for biomarkers detection. *Biosens. Bioelectron.* **2021**, *184*, 113252.
(11) Owicki, J. C.; Bousse, L. J.; Hafeman, D. G.; Kirk, G. L.; Olson, J. D.; Wada, H. G.; Parce, J. W. The Light-addressable potentiometric sensor: principles and biological applications. *Annu. Rev. Biophys. Biomol. Struct.* **1994**, *23*, 87−113.
(12) Meng, Y.; Chen, F. M.; Wu, C. S.; Krause, S.; Wang, J.; Zhang, D. W. Light-Addressable Electrochemical Sensors toward Spatially Resolved Biosensing and Imaging Applications. *ACS Sens.* **2022**, *7*, 1791−1807.
(13) Yoshinobu, T.; Schoening, M. J. Light-addressable potentiometric sensors for cell monitoring and biosensing. *Curr. Opin. Electrochem.* **2021**, *28*, 100727.
(14) Zhang, W.; Liu, C.; Zou, X. B.; Zhang, H.; Xu, X. C. Micrometer-scale light-addressable potentiometric sensor on an optical fiber for biological glucose determination. *Anal. Chim. Acta* **2020**, *1123*, 36−43.
(15) Li, G. Y.; Li, W. Z.; Li, S. S.; Shi, X. H.; Liang, J. T.; Lai, J. X.; Zhou, Z. D. A novel aptasensor based on light-addressable potentiometric sensor for the determination of Alpha-fetoprotein. *Biochem. Eng. J.* **2020**, *164*, 107780.
(16) Shaibani, P. M.; Etayash, H.; Jiang, K.; Sohrabi, A.; Hassanpourfard, M.; Naicker, S.; Sadrzadeh, M.; Thundat, T. Portable Nanofiber-Light Addressable Potentiometric Sensor for Rapid Escherichia coli Detection in Orange Juice. *ACS Sens.* **2018**, *3*, 815−822.
(17) Dantism, S.; Roehlen, D.; Selmer, T.; Wagner, T.; Wagner, P.; Schoening, M. J. Quantitative differential monitoring of the metabolic activity of Corynebacterium glutamicum cultures utilizing a light addressable potentiometric sensor system. *Biosens. Bioelectron.* **2019**, *139*, 111332.
(18) Shaibani, P. M.; Jiang, K. R.; Haghighat, G.; Hassanpourfard, M.; Etayash, H.; Naicker, S.; Thundat, T. The detection of Escherichia coli (E. coli) with the pH sensitive hydrogel nanofiber-light addressable potentiometric sensor (NF-LAPS). *Sens. Actuator B* **2016**, *226*, 176−183.
(19) Hu, N.; Zhou, J.; Su, K. Q.; Zhang, D. M.; Xiao, L. D.; Wang, T. X.; Wang, P. An integrated label-free cell-based biosensor for simultaneously monitoring of cellular physiology multiparameter in vitro. *Biomed. Microdevices* **2013**, *15*, 473−480.
(20) Gu, Y. J.; Ju, C.; Li, Y. J.; Shang, Z. Q.; Wu, Y. D.; Jia, Y. F.; Niu, Y. J. Detection of circulating tumor cells in prostate cancer based on carboxylated graphene oxide modified light addressable potentiometric sensor. *Biosens. Bioelectron.* **2015**, *66*, 24−31.
(21) Stein, B.; George, M.; Gaub, H. E.; Parak, W. J. Extracellular measurements of averaged ionic currents with the light-addressable potentiometric sensor (LAPS). *Sens. Actuators, B* **2004**, *98*, 299−304.
(22) Liang, T.; Gu, C. L.; Gan, Y.; Wu, Q.; He, C. J.; Tu, J. W.; Pan, Y. X.; Qiu, Y.; Kong, L. B.; Wan, H.; Wang, P. Microfluidic chip system integrated with light addressable potentiometric sensor (LAPS) for real-time extracellular acidification detection. *Sens. Actuators, B* **2019**, *301*, 127004.
(23) Zhang, W.; Xu, Y. W.; Zou, X. B. Rapid determination of cadmium in rice using an all-solid RGO-enhanced light addressable potentiometric sensor. *Food Chem.* **2018**, *261*, 1−7.
(24) Arora, P.; Sindhu, A.; Dilbaghi, N.; Chaudhury, A. Biosensors as innovative tools for the detection of food borne pathogens. *Biosens. Bioelectron.* **2011**, *28*, 1−12.
(25) Liu, Q. J.; Yu, H.; Tan, Z.; Cai, H.; Ye, W. W.; Zhang, M.; Wang, P. In vitro assessing the risk of drug-induced cardiotoxicity by embryonic stem cell-based biosensor. *Sens. Actuators, B* **2011**, *155*, 214−219.
(26) Shaibani, P. M.; Etayash, H.; Naicker, S.; Kaur, K.; Thundat, T. Metabolic Study of Cancer Cells Using a pH Sensitive Hydrogel Nanofiber Light Addressable Potentiometric Sensor. *ACS Sens.* **2017**, *2*, 151−156.
(27) Xiao, W. X.; Chen, Z. C.; Jiang, X. G.; Zhao, H. T.; Chu, F. G.; Hou, H. B. A taste sensor based on surface imprinted TiO_2 membrane. *Tenth International Conference on Photonics and Imaging in Biology and Medicine*; SPIE, 2012; Vol. *8329*, p 83290W. DOI: 10.1117/12.922998.
(28) Du, L. P.; Wang, J.; Chen, W.; Zhao, L. H.; Wu, C. S.; Wang, P. Dual functional extracellular recording using a light-addressable potentiometric sensor for bitter signal transduction. *Anal. Chim. Acta* **2018**, *1022*, 106−112.
(29) Zhang, W.; Xu, Y. W.; Tahir, H. E.; Zou, X. B.; Wang, P. Rapid and wide-range determination of Cd(II), Pb(II), Cu(II) and Hg(II) in fish tissues using light addressable potentiometric sensor. *Food Chem.* **2017**, *221*, 541−547.
(30) Ha, D.; Hu, N.; Wu, C. X.; Kirsanov, D.; Legin, A.; Khaydukova, M.; Wang, P. Novel structured light-addressable potentiometric sensor array based on PVC membrane for determination of heavy metals. *Sens. Actuators, B* **2012**, *174*, 59−64.
(31) Hafeman, D. G.; Parce, J. W.; Mcconnell, H. M. Light-addressable potentiometric sensor for biochemical systems. *Science* **1988**, *240*, 1182−1185.
(32) Jia, Y. F.; Yin, X. B.; Zhang, J.; Zhou, S.; Song, M.; Xing, K. L. Graphene oxide modified light addressable potentiometric sensor and its application for ssDNA monitoring. *Analyst* **2012**, *137*, 5866−5873.
(33) Tu, Y.; Ahmad, N.; Briscoe, J.; Zhang, D. W.; Krause, S. Light-Addressable Potentiometric Sensors Using ZnO Nanorods as the Sensor Substrate for Bioanalytical Applications. *Anal. Chem.* **2018**, *90*, 8708−8715.
(34) Zhao, W. B.; Liu, S. B.; Tan, J.; Luo, J. Z.; Chen, Y. H.; Li, G. F.; Li, Y. B. Urease-modified LAPS: Two-dimensional dynamic

https://doi.org/10.1021/acsomega.3c04789
ACS Omega 2023, 8, 42028−42044

detection of enzymatic reactions. *J. Electroanal. Chem.* **2022**, *922*, 116803.
(35) Liang, J. T.; Shi, X. H.; Feng, H. F.; Chen, M.; Li, W. Z.; Lai, J. X.; Hu, W. P.; Li, G. Y. 1,5-anhydroglucitol biosensor based on light-addressable potentiometric sensor with RGO-CS-Fc/Au NPs nano-hybrids. *Bioelectrochemistry* **2021**, *142*, 107938.
(36) Wu, C. S.; Du, L. P.; Zou, L.; Zhao, L. H.; Wang, P. An ATP sensitive light addressable biosensor for extracellular monitoring of single taste receptor cell. *Biomed. Microdevices* **2012**, *14*, 1047−1053.
(37) Liu, Q. J.; Ye, W. W.; Yu, H.; Hu, N.; Du, L. P.; Wang, P.; Yang, M. Olfactory mucosa tissue-based biosensor: A bioelectronic nose with receptor cells in intact olfactory epithelium. *Sens. Actuators, B* **2010**, *146*, 527−533.
(38) Liu, Q. J.; Ye, W. W.; Hu, N.; Cai, H.; Yu, H.; Wang, P. Olfactory receptor cells respond to odors in a tissue and semi-conductor hybrid neuron chip. *Biosens. Bioelectron.* **2010**, *26*, 1672−1678.
(39) Dantism, S.; Takenaga, S.; Wagner, T.; Wagner, P.; Schoening, M. J. Differential imaging of the metabolism of bacteria and eukaryotic cells based on light-addressable potentiometric sensors. *Electrochim. Acta* **2017**, *246*, 234−241.
(40) Dantism, S.; Takenaga, S.; Wagner, T.; Wagner, P.; Schoening, M. J. Light-addressable potentiometric sensor (LAPS) combined with multi-chamber structures to investigate the metabolic activity of cells. *Procedia Eng.* **2015**, *120*, 384−387 (Eurosensors 2015 Conference)..
(41) Werner, C. F.; Groebel, S.; Krumbe, C.; Wagner, T.; Selmer, T.; Yoshinobu, T.; Baumann, M. E. M.; Keusgen, M.; Schoening, M. J. Nutrient concentration-sensitive microorganism-based biosensor. *Phys. Status Solidi A* **2012**, *209* (5), 900−904.
(42) Wu, C. S.; Bronder, T.; Poghossian, A.; Werner, C. F.; Baecker, M.; Schoening, M. J. Label-free electrical detection of DNA with a multi-spot LAPS: First step towards light-addressable DNA chips. *Phys. Status Solidi A* **2014**, *211*, 1423−1428.
(43) Luo, J. Z.; Liu, S. B.; Tan, J.; Chen, Y. H.; Zhao, W. B.; Li, H. J.; Li, G. F.; Du, Y. Q. A differential light addressable potentiometric sensor using solid-state reference. *Electrochim. Acta* **2023**, *438*, 141542.
(44) Krause, S.; Talabani, H.; Xu, M.; Moritz, W.; Griffiths, J. Scanning photo-induced impedance microscopy - an impedance based imaging technique. *Electrochim. Acta* **2002**, *47*, 2143−2148.
(45) Zhang, D. W.; Wu, F.; Krause, S. LAPS and SPIM Imaging Using ITO-Coated Glass as the Substrate Material. *Anal. Chem.* **2017**, *89*, 8129−8133.
(46) Miyamoto, K.; Yu, B.; Isoda, H.; Wagner, T.; Schoening, M. J.; Yoshinobu, T. Visualization of the recovery process of defects in a cultured cell layer by chemical imaging sensor. *Sens. Actuators, B* **2016**, *236*, 965−969.
(47) Wu, F.; Zhou, B.; Wang, J.; Zhong, M. C.; Das, A.; Watkinson, M.; Hing, K.; Zhang, D. W.; Krause, S. Photoelectrochemical Imaging System for the Mapping of Cell Surface Charges. *Anal. Chem.* **2019**, *91*, 5896−5903.
(48) Zhou, B.; Das, A.; Zhong, M. C.; Guo, Q.; Zhang, D. W.; Hing, K. A.; Sobrido, A. J.; Titirici, M. M.; Krause, S. Photoelectrochemical imaging system with high spatiotemporal resolution for visualizing dynamic cellular responses. *Biosens. Bioelectron.* **2021**, *180*, 113121.
(49) Wang, J.; Tian, Y. L.; Chen, F. M.; Chen, W.; Du, L. P.; He, Z. Y.; Wu, C. S.; Zhang, D. W. Scanning Electrochemical Photometric Sensors for Label-Free Single-Cell Imaging and Quantitative Absorption Analysis. *Anal. Chem.* **2020**, *92*, 9739−9744.
(50) Wang, J.; Chen, F. M.; Guo, Q.; Meng, Y.; Jiang, M. R.; Wu, C. S.; Zhuang, J.; Zhang, D. W. Light-Addressable Square Wave Voltammetry (LASWV) Based on a Field-Effect Structure for Electrochemical Sensing and Imaging. *ACS Sens.* **2021**, *6*, 1636−1642.
(51) Nakao, M.; Yoshinobu, T.; Iwasaki, H. Scanning-laser-beam semiconductor pH-imaging sensor. *Sens. Actuators, B* **1994**, *20*, 119−123.
(52) Wagner, T.; Werner, C. F.; Miyamoto, K.; Schoning, M. J.; Yoshinobu, T. Development and characterisation of a compact light-addressable potentiometric sensor (LAPS) based on the digital light processing (DLP) technology for flexible chemical imaging. *Sens. Actuators, B* **2012**, *170*, 34−39.
(53) Peng, H. Y.; Yang, C. Y.; Chen, Y. P.; Liu, H. L.; Chen, T. C.; Pijanowska, D. G.; Chu, P. Y.; Hsieh, C. H.; Wu, M. H. An integrated actuating and sensing system for light-addressable potentiometric sensor (LAPS) and light-actuated AC electroosmosis (LACE) operation. *Biomicrofluidics* **2021**, *15*, 024109.
(54) Lin, Y. H.; Das, A.; Lai, C. S. A simple and convenient set-up of light addressable potentiometric sensors (LAPS) for chemical imaging using a commercially available pojector as a light source. *Int. J. Electrochem. Sci.* **2013**, *8*, 7062−7074.
(55) Miyamoto, K.; Kaneko, K.; Matsuo, A.; Wagner, T.; Kanoha, S.; Schoning, M. J.; Yoshinobu, T. Miniaturized chemical imaging sensor system using an OLED display panel. *Procedia Eng.* **2010**, *5*, 516−519.
(56) Werner, C. F.; Wagner, T.; Miyamoto, K.; Yoshinobu, T.; Schoeninig, M. J. High speed and high resolution chemical imaging based on a new type of OLED-LAPS set-up. *Procedia Eng.* **2011**, *25*, 346−349.
(57) Das, A.; Chen, T. C.; Lin, Y. T.; Lai, C. S.; Yuan, H. L.; Yang, C. M. Ultra-high scanning speed chemical image sensor based on light addressable potentiometric sensor with analog micro-mirror. *2013 IEEE Sens. Proc.* **2013**, 1412−1415.
(58) Das, A.; Chen, T. C.; Yang, C. M.; Lai, C. S. A high-speed, flexible-scanning chemical imaging system using a light-addressable potentiometric sensor integrated with an analog micromirror. *Sens. Actuator B-Chem.* **2014**, *198*, 225−232.
(59) Wagner, T.; Werner, C. F. B.; Miyamoto, K.-I.; Schoning, M. J.; Yoshinobu, T. A high-density multi-point LAPS set-up using a VCSEL array and FPGA control. *Sens. Actuators, B* **2011**, *154*, 124−128.
(60) Sartore, M.; Adami, M.; Nicolini, C.; Bousse, L.; Mostarshed, S.; Hafeman, D. Minority carrier diffusion length effects on light-addressable potentiometric sensor (LAPS) devices. *Sens. Actuator A-Phys.* **1992**, *32*, 431−436.
(61) Itabashi, A.; Kosaka, N.; Miyamoto, K.; Wagner, T.; Schoning, M. J.; Yoshinobu, T. High-speed chemical imaging system based on front-side-illuminated LAPS. *Sens. Actuator B-Chem.* **2013**, *182*, 315−321.
(62) Guo, Y.; Werner, C. F.; Canales, A.; Yu, L.; Jia, X.; Anikeeva, P.; Yoshinobu, T. Polymer-fiber-coupled field-effect sensors for label-free deep brain recordings. *PLoS One* **2020**, *15*, e0228076.
(63) Miyamoto, K.; Itabashi, A.; Wagner, T.; Schoning, M. J.; Yoshinobu, T. High-speed chemical imaging inside a microfluidic channel. *Sens. Actuators. B* **2014**, *194*, 521−527.
(64) Li, X. L.; Liu, S. B.; Fan, P. P.; Werner, C. F.; Miyamoto, K.; Yoshinobu, T. A bubble-assisted electroosmotic micropump for a delivery of a droplet in a microfluidic channel combined with a light-addressable potentiometric sensor. *Sens. Actuators, B* **2017**, *248*, 993−997.
(65) Truong, H. A.; Werner, C. F.; Miyamoto, K.; Yoshinobu, T. A Partially Etched Structure of Light-Addressable Potentiometric Sensor for High-Spatial-Resolution and High-Speed Chemical Imaging. *Phys. Status Solidi A* **2018**, *215*, 1700964.
(66) Yang, C. M.; Liao, Y. H.; Chen, C. H.; Chen, T. C.; Lai, C. S.; Pijanowska, D. G. P-I-N amorphous silicon for thin-film light-addressable potentiometric sensors. *Sens. Actuators, B* **2016**, *236*, 1005−1010.
(67) Yang, C. M.; Chen, C. H.; Chang, L. B.; Lai, C. S. IGZO Thin-Film Light-Addressable Potentiometric Sensor. *IEEE Electron. Device L.* **2016**, *37*, 1481−1484.
(68) Nakao, M.; Inoue, S.; Oishi, R.; Yoshinobu, T.; Iwasaki, H. Observation of Microorganism Colonies Using a Scanning-Laser-Beam pH-Sensing Microscope. *J. Ferment. Bioeng.* **1995**, *79*, 163−166.
(69) Hiraishi, N.; Kitasako, Y.; Nikaido, T.; Foxton, R. M.; Tagami, J.; Nomura, S. Acidity of conventional luting cements and their diffusion through bovine dentine. *Int. Endod. J.* **2003**, *36*, 622−628.
(70) Miyamoto, K.; Sakakita, S.; Wagner, T.; Schoening, M. J.; Yoshinobu, T. Application of chemical imaging sensor to in-situ pH imaging in the vicinity of a corroding metal surface. *Electrochim. Acta* **2015**, *183*, 137−142.

https://doi.org/10.1021/acsomega.3c04789
ACS Omega 2023, 8, 42028−42044

(71) Miyamoto, K.; Sakakita, S.; Werner, C. F.; Yoshinobu, T. A Modified Chemical Imaging Sensor System for Real-Time pH Imaging of Accelerated Crevice Corrosion of Stainless Steel. *Phys. Status Solidi A* **2018**, *215*, 1700963.
(72) Miyamoto, K.; Hiramitsu, R.; Werner, C. F.; Yoshinobu, T. Simultaneous In Situ Imaging of pH and Surface Roughening during the Progress of Crevice Corrosion of Stainless Steel. *Sensors* **2022**, *22*, 2246.
(73) Miyamoto, K.; Kaneko, M.; Wang, M.; Werner, C. F.; Yoshinobu, T. Detection of hydrogen permeation through pure iron with light-addressable potentiometric sensor. *ISIJ Int.* **2021**, *61*, 1330−1332.
(74) Lee, C. S.; Kim, S. K.; Kim, M. Ion-Sensitive Field-Effect Transistor for Biological Sensing. *Sensors* **2009**, *9*, 7111−7131.
(75) Guo, Y. Y.; Werner, C. F.; Handa, S.; Wang, M. Y.; Ohshiro, T.; Mushiake, H.; Yoshinobu, T. Miniature multiplexed label-free pH probe *in vivo*. *Biosens. Bioelectron.* **2021**, *174*, 112870.
(76) Chen, L.; Zhou, Y. L.; Jiang, S. H.; Kunze, J.; Schmuki, P.; Krause, S. High resolution LAPS and SPIM. *Electrochem. Commun.* **2010**, *12*, 758−760.
(77) Wang, J.; Zhou, Y. L.; Watkinson, M.; Gautrot, J.; Krause, S. High-sensitivity light-addressable potentiometric sensors using silicon on sapphire functionalized with self-assembled organic monolayers. *Sens. Actuators, B* **2015**, *209*, 230−236.
(78) Ito, Y. High-spatial resolution LAPS. *Sens. Actuators, B* **1998**, *52*, 107−111.
(79) Tan, J.; Liu, S. B.; Luo, J. Z.; Chen, Y. H.; Zhao, W. B.; Li, H. J.; Li, G. F.; Li, X. L. Light addressable potentiometric sensor with well-ordered pyramidal pits-patterned silicon. *Anal. Chim. Acta* **2023**, *1238*, 340599.
(80) Tan, J.; Liu, S. B.; Luo, J. Z.; Li, H. J.; Chen, Y. H.; Du, Y. Q.; Li, X. L. Honeycomb meshed working electrodes based on microsphere lithography for high-resolution chemical image sensor. *Anal. Chim. Acta* **2021**, *1178*, 338798.
(81) Nii, K.; Inami, W.; Kawata, Y. High Spatial Resolution Ion Imaging by Focused Electron-Beam Excitation with Nanometric Thin Sensor Substrate. *Sensors.* **2022**, *22*, 1112.
(82) Guo, Y. Y.; Miyamoto, K.; Wagner, T.; Schoening, M. J.; Yoshinobu, T. Device simulation of the light-addressable potentiometric sensor for the investigation of the spatial resolution. *Sens. Actuators, B* **2014**, *204*, 659−665.
(83) Yoshinobu, T.; Miyamoto, K.; Wagner, T.; Schoening, M. J. Recent developments of chemical imaging sensor systems based on the principle of the light-addressable potentiometric sensor. *Sens. Actuators, B* **2015**, *207*, 926−932.
(84) Parak, W. J.; Hofmann, U. G.; Gaub, H. E.; Owicki, J. C. Lateral resolution of light-addressable potentiometric sensors: an experimental and theoretical investigation. *Sens. Actuators, A* **1997**, *63*, 47−57.
(85) George, M.; Parak, W. J.; Gerhardt, I.; Moritz, W.; Kaesen, F.; Geiger, H.; Eisele, I.; Gaub, H. E. Investigation of the spatial resolution of the light-addressable potentiometric sensor. *Sens. Actuators, A* **2000**, *86*, 187−196.
(86) Nakao, M.; Inoue, S.; Yoshinobu, T.; Iwasaki, H. High-resolution pH imaging sensor for microscopic observation of microorganisms. *Sens. Actuators, B* **1996**, *34*, 234−239.
(87) Chen, D.; Liu, S. B.; Yin, S. M.; Liang, J. T. Light-addressable potentiometric sensor with the micro blind holes substrate. *IET Sci., Meas. Technol.* **2017**, *11*, 57−62.
(88) Truong, H. A.; Werner, C. F.; Miyamoto, K.; Yoshinobu, T. Multi-Well Sensor Platform Based on a Partially Etched Structure of a Light-Addressable Potentiometric Sensor. *Phys. Status Solidi A* **2019**, *216*, 1800764.
(89) Yang, C. M.; Zeng, W. Y.; Chen, C. H.; Chen, Y. P.; Chen, T. C. Spatial resolution and 2D chemical image of light-addressable potentiometric sensor improved by inductively coupled-plasma reactive-ion etching. *Sens. Actuators, B* **2018**, *258*, 1295−1301.
(90) Zeng, W. Y.; Chen, T. C.; Liu, H. L.; Chen, Y. P.; Yang, C. M. Thin silicon light-addressable potentiometric sensor by deep reactive-ion etching*19th International Conference on Solid-State Sensors, Actuators and Microsystems (TRANSDUCERS)*; IEEE, 2017; pp 1540−1542..
(91) Krause, S.; Moritz, M.; Talabani, H.; Xu, M.; Sabot, A.; Ensell, G. Scanning Photo-Induced Impedance Microscopy—Resolution studies and polymer characterization. *Electrochim. Acta* **2006**, *51*, 1423−1430.
(92) Moritz, W.; Gerhardt, I.; Roden, D.; Xu, M.; Krause, S. Photocurrent measurements for laterally resolved interface characterization. *Fresenius' J. Anal Chem.* **2000**, *367*, 329−333.
(93) Moritz, W.; Yoshinobu, T.; Finger, F.; Krause, S.; Martin-Fernandez, M.; Schoening, M. J. High resolution LAPS using amorphous silicon as the semiconductor material. *Sens. Actuators, B* **2004**, *103*, 436−441.
(94) Das, A.; Lin, Y. H.; Lai, C. S. Miniaturized amorphous-silicon based chemical imaging sensor system using a mini-projector as a simplified light-addressable scanning source. *Sens. Actuators, B* **2014**, *190*, 664−672.
(95) Li, Y. C.; Jiao, B.; Zhang, Y. J.; Wang, J.; Ren, W.; Zhang, D. W.; Hou, X.; Wu, Z. X. Bipolar Light-Addressable Potentiometric Sensor Based on Fullerene Photosensitive Layer. *Adv. Mater. Technol.* **2021**, *6*, 2001221.
(96) Yang, C. M.; Chen, C. H.; Akuli, N.; Yen, T. H.; Lai, C. S. A revised manuscript submitted to sensors and actuators B: Chemical illumination modification from an LED to a laser to improve the spatial resolution of IGZO thin film light-addressable potentiometric sensors in pH detections. *Sens. Actuators, B* **2021**, *329*, 128953.
(97) Zhou, B.; Das, A.; Kappers, M. J.; Oliver, R. A.; Humphreys, C. J.; Krause, S. InGaN as a Substrate for AC Photoelectrochemical Imaging. *Sensors* **2019**, *19*, 4386.
(98) Yang, C. M.; Liao, Y. H.; Chen, C. H.; Chen, C. C.; Lai, C. S. P-I-N Amorphous Silicon Light-Addressable Potentiometric Sensors for High-photovoltage Chemical Image. *Procedia Eng.* **2015**, *120*, 1015−1018.
(99) Guo, Y.; Seki, K.; Miyamoto, K.-i.; Wagner, T.; Schoning, M. J.; Yoshinobu, T. Novel photoexcitation method for light-addressable potentiometric sensor with higher spatial resolution. *Appl. Phys. Express* **2014**, *7*, 067301.
(100) Guo, Y. Y.; Seki, K.; Miyamoto, K.; Wagner, T.; Schoening, M. J.; Yoshinobu, T. Device simulation of the light-addressable potentiometric sensor with a novel photoexcitation method for a higher spatial resolution. *Procedia Eng.* **2014**, *87*, 456−459.
(101) Miyamoto, K.; Seki, K.; Guo, Y. Y.; Wagner, T.; Schoening, M. J.; Yoshinobu, T. Enhancement of the Spatial Resolution of the Chemical Imaging Sensor by a Hybrid Fiber-Optic Illumination. *Procedia Eng.* **2014**, *87*, 612−625.
(102) Miyamoto, K.; Seki, K.; Suto, T.; Werner, C. F.; Wagner, T.; Schoening, M. J.; Yoshinobu, T. Improved spatial resolution of the chemical imaging sensor with a hybrid illumination that suppresses lateral diffusion of photocarriers. *Sens. Actuators, B* **2018**, *273*, 1328−1333.
(103) Werner, C. F.; Miyamoto, K.; Wagner, T.; Schoening, M. J.; Yoshinobu, T. Lateral resolution enhancement of pulse-driven light-addressable potentiometric sensor. *Sens. Actuators, B* **2017**, *248*, 961−965.
(104) Shibano, S.; Kawata, Y.; Inami, W. Evaluation of pH Measurement Using Electron-Beam-Induced Current Detection. *Phys. Status Solidi A* **2021**, *218*, 2100147.
(105) Zhang, D. W.; Wu, F.; Wang, J.; Watkinson, M.; Krause, S. Image detection of yeast *Saccharomyces cerevisiae* by light-addressable potentiometric sensors (LAPS). *Electrochem. Commun.* **2016**, *72*, 41−45.
(106) Jacques, R.; Zhou, B.; Marhuenda, E.; Gorecki, J.; Das, A.; Iskratsch, T.; Krause, S. Photoelectrochemical imaging of single cardiomyocytes and monitoring of their action potentials through contact force manipulation of organoids. *Biosens. Bioelectron.* **2023**, *223*, 115024.
(107) Chen, F. M.; Yang, Q. Y.; Jiang, M. R.; Meng, Y.; Zhang, D. W.; Wang, J. Visualization of electrochemical reactions on micro-

https://doi.org/10.1021/acsomega.3c04789
ACS Omega 2023, 8, 42028−42044

electrodes using light-addressable potentiometric sensor imaging. *Anal. Chim. Acta* **2022**, *1224*, 340237.
(108) Miyamoto, K.; Ichimura, H.; Wagner, T.; Schoening, M. J.; Yoshinobu, T. Chemical imaging of the concentration profile of ion diffusion in a microfluidic channel. *Sens. Actuators, B* **2013**, *189*, 240−245.
(109) Miyamoto, K.; Hirayama, Y.; Wagner, T.; Schoening, M. J.; Yoshinobu, T. Visualization of enzymatic reaction in a microfluidic channel using chemical imaging sensor. *Electrochim. Acta* **2013**, *113*, 768−772.
(110) Welden, R.; Jablonski, M.; Wege, C.; Keusgen, M.; Wagner, P. H.; Wagner, T.; Schoening, M. J. Light-addressable actuator-sensor platform for monitoring and manipulation of pH gradients in microfluidics: a case study with the enzyme penicillinase. *Biosensors (Basel)* **2021**, *11*, 171.
(111) Ozsoylu, D.; Isik, T.; Demir, M. M.; Schoning, M. J.; Wagner, T. Cryopreservation of a cell-based biosensor chip modified with elastic polymer fibers enabling ready-to-use on-site applications. *Biosens. Bioelectron.* **2021**, *177*, 112983.

https://doi.org/10.1021/acsomega.3c04789
ACS Omega 2023, 8, 42028−42044